Geochemistry Geophysics Geosystems G3
AN ELECTRONIC JOURNAL OF THE EARTH SCIENCES
Published by AGU and the Geochemical Society

Article
Volume 7, Number 5
2 May 2006
Q05001, doi:10.1029/2005GC001086
ISSN: 1525-2027

Submarine radial vents on Mauna Loa Volcano, Hawai`i

V. Dorsey Wanless and M. O. Garcia
Department of Geology and Geophysics, University of Hawai`i, Honolulu, Hawaii 96822, USA (vdorseyw@yahoo.com)

F. A. Trusdell
Hawaiian Volcano Observatory, U.S. Geological Survey, Hawai`i National Park, Hawaii 96718, USA

J. M. Rhodes
Department of Geosciences, University of Massachusetts, Amherst, Massachusetts 01003, USA

M. D. Norman
Research School of Earth Sciences, Australian National University, Canberra, ACT 0200, Australia

Dominique Weis
Department of Earth and Ocean Sciences, University of British Columbia, Vancouver, BC, Canada V6T 1Z4

D. J. Fornari and M. D. Kurz
Woods Hole Oceanographic Institution, Woods Hole, Massachusetts 02543, USA

Hervé Guillou
Laboratorie des Sciences du Climat et de l'Environnement Domaine du CNRS, F-91198 Gif sur Yvette, France

[1] A 2002 multibeam sonar survey of Mauna Loa's western flank revealed ten submarine radial vents and three submarine lava flows. Only one submarine radial vent was known previously. The ages of these vents are constrained by eyewitness accounts, geologic relationships, Mn-Fe coatings, and geochemical stratigraphy; they range from 128 years B.P. to possibly 47 ka. Eight of the radial vents produced degassed lavas despite eruption in water depths sufficient to inhibit sulfur degassing. These vents formed truncated cones and short lava flows. Two vents produced undegassed lavas that created "irregular" cones and longer lava flows. Compositionally and isotopically, the submarine radial vent lavas are typical of Mauna Loa lavas, except two cones that erupted alkalic lavas. He-Sr isotopes for the radial vent lavas follow Mauna Loa's evolutionary trend. The compositional and isotopic heterogeneity of these lavas indicates most had distinct parental magmas. Bathymetry and acoustic backscatter results, along with photography and sampling during four JASON2 dives, are used to produce a detailed geologic map to evaluate Mauna Loa's submarine geologic history. The new map shows that the 1877 submarine eruption was much larger than previously thought, resulting in a 10% increase for recent volcanism. Furthermore, although alkalic lavas were found at two radial vents, there is no systematic increase in alkalinity among these or other Mauna Loa lavas as expected for a dying volcano. These results refute an interpretation that Mauna Loa's volcanism is waning. The submarine radial vents and flows cover 29 km^2 of seafloor and comprise a total volume of $\sim 2 \times 10^9$ m^3 of lava, reinforcing the idea that submarine lava eruptions are important in the growth of oceanic island volcanoes even after they emerged above sea level.

Components: 17,486 words, 16 figures, 7 tables.

Keywords: Hawaii; Mauna Loa; submarine volcanism; radial vents; bathymetry; igneous petrology.

Index Terms: 1065 Geochemistry: Major and trace element geochemistry; 3045 Marine Geology and Geophysics: Seafloor morphology, geology, and geophysics; 8427 Volcanology: Subaqueous volcanism; 1040 Geochemistry: Radiogenic isotope geochemistry; 3075 Marine Geology and Geophysics: Submarine tectonics and volcanism.

Received 23 July 2005; **Revised** 24 October 2005; **Accepted** 12 December 2005; **Published** 2 May 2006.

Wanless, V. D., M. O. Garcia, F. A. Trusdell, J. M. Rhodes, M. D. Norman, D. Weis, D. J. Fornari, M. D. Kurz, and H. Guillou (2006), Submarine radial vents on Mauna Loa Volcano, Hawai'i, *Geochem. Geophys. Geosyst.*, *7*, Q05001, doi:10.1029/2005GC001086.

1. Introduction

[2] Mauna Loa, the largest volcano on earth (80,000 km^3 [*Robinson and Eakins*, 2006]), generally erupts from its two rift zones and summit area [*Barnard*, 1995]. Unlike other Hawaiian shield volcanoes, it also erupts along radial vents located outside of these regions [e.g., *Lockwood and Lipman*, 1987]. Mauna Loa's subaerial radial vents span a narrow age range (147 years to ~4 ka) [*Lockwood and Lipman*, 1987] reflecting the volcano's relatively high eruption frequency (39 eruptions since 1832, the start of its historical record) [*Barnard*, 1995]. Radial vents are thought to result from the injection of magma into the center of an axisymetric volcano, if there are no external stresses acting on the volcano [*Pollard*, 1987; *Walker*, 1993]. They are prominent features at several isolated volcanoes including the Spanish Peaks [*Ode*, 1957] and the Galápagos Islands [*Chadwick and Howard*, 1991; *Naumann and Geist*, 2000]. Mauna Loa is not isolated; it grew on the flanks of two older, now dormant volcanoes (Mauna Kea and Hualālai) and a younger volcano (Kīlauea) is growing on its southeast flank (Figure 1). The enormous size of the Mauna Loa combined with the proximity of neighboring shield volcanoes creates a complicated stress field allowing formation of both rift zones and radial vents [e.g., *Fiske and Jackson*, 1972; *Swanson et al.*, 1976; *Lipman*, 1980].

[3] Forty-four subaerial radial vent eruptions have been identified on the northern and western flanks of Mauna Loa (Figure 1). Only one submarine radial vent, active in 1877 [*Whitney*, 1877], had been mapped prior to our study. Four additional submarine radial vents were suggested but not surveyed by *Davis et al.* [2003], so their existence was uncertain. We identified nine new submarine radial vents and three lava flow fields in an area thought to consist primarily of fragmental debris [*Moore and Chadwick*, 1995]. These new vents greatly expand the known area affected by this type of volcanism and highlight the importance of radial vent volcanism in the submarine growth of Mauna Loa and other oceanic island volcanoes. No existing model adequately explains the origin of radial vents. Although it is beyond the scope of this paper to address the origin of Mauna Loa's radial vents, any viable new model for their formation must now also account for the nine new submarine radial vents.

[4] Here we present a new geologic map of the submarine Kealakekua Bay area based on high-resolution multibeam echo sounding (EM300), and photography and sampling by the JASON2 remotely operated vehicle (ROV). Volume estimates are made for the submarine radial vents and associated lava flows to determine their importance on the volcano's growth. The shapes of these cones are compared to other Hawaiian submarine cones to better understand their formation. Glass S content is found to be higher in flows with lengths longer than 3 km. Two of the submarine radial vents erupted alkalic lavas, the first lavas of this composition to be sampled from Mauna Loa. The petrology of the alkalic lavas are discussed separately [*Wanless et al.*, 2006]. Here, their geology and geochemistry are compared to those of eight tholeiitic submarine radial vent eruptions (including the 1877 vent) to evaluate the geologic history on Mauna Loa's submarine west flank.

2. Mauna Loa's Radial Vents: Definitions, Eruptions, and Models

2.1. Radial Vent Definition

[5] Mauna Loa's radial vent population is defined here as all vents located outside the volcano's summit and rift zone regions that are oriented radially to the summit caldera. If multiple fissures were produced during a single event, they are considered part of one radial vent eruption. This definition differs somewhat from that of *Lockwood and Lipman* [1987] in that they counted all eruptions that occurred outside the summit and two rift zone regions, regardless of fissure orientation. Twelve of the 66 radial vents they identified are related to northeast rift zone eruptions and are oriented orthogonal to the rift zone, not radial to the summit caldera. These vents are not included in our radial vent count. *Lockwood and Lipman* [1987] also counted multiple fissures produced during a single eruption as separate radial vents.

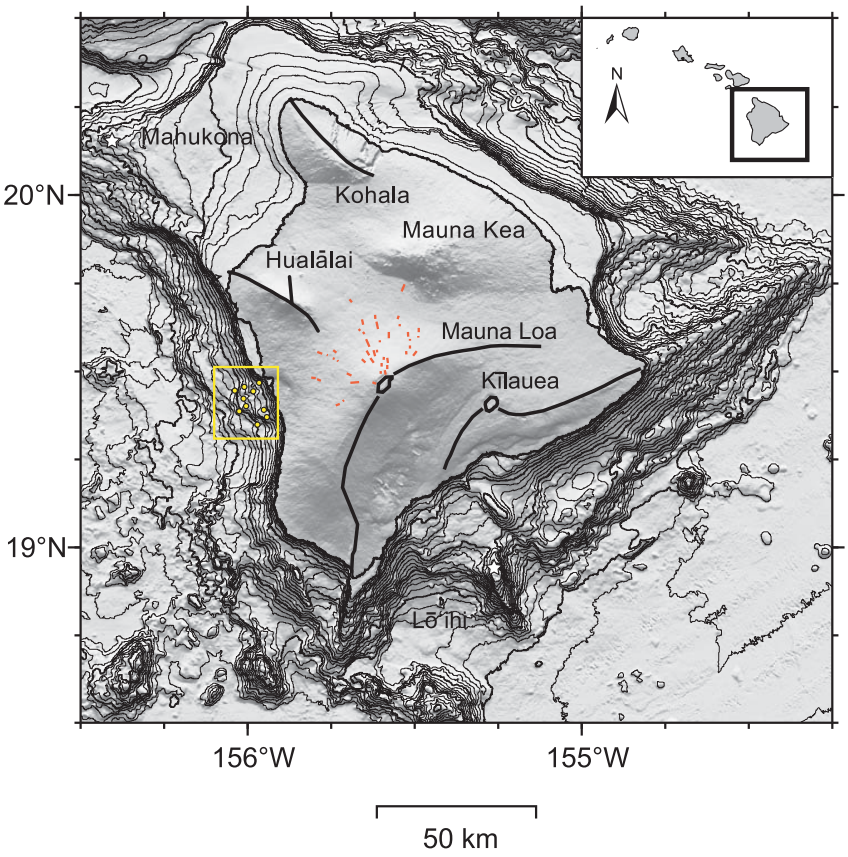

Figure 1. Shaded relief map of the island of Hawai`i, its flanks and the surrounding seafloor showing five subaerial shield volcanoes, with their rift zones marked by thick black lines, and two submarine volcanoes (stars). The bathymetric contour interval is 100 m, with 1000 m contours shown as heavier lines. Mauna Loa's 44 subaerial radial vents are shown as short orange dashes on its northern and western flanks. The locations of the 10 submarine radial vents are noted by yellow circles. The yellow rectangle indicates the survey and sampling area adjacent to Kealakekua Bay.

Using our definition, Mauna Loa has had 44 subaerial radial vent eruptions over the last ~2,000 years.

2.2. Post-1832 Radial Vent Eruptions

[6] Three radial vent eruptions have occurred since 1832 (1852, 1859, and 1877) [*Barnard*, 1995]. These eruptions occurred during a period of relatively high eruption rates on the volcano [*Lipman*, 1995]. The 1852 eruption had a short phase of radial vent activity that was followed by a much larger northeastern rift zone eruption. The 1852 radial fissure broke out at 3,920 m above sea level and produced a lava flow that traveled ~5 km down the northwestern flank of the volcano. The 1859 radial eruption began after a <1 day summit eruption [*Barnard*, 1995]. Lava issued from multiple vents, ranging from 3,375 m to 2,630 m above sea level [*Stearns and Macdonald*, 1946]. This eruption lasted for ~300 days [*Barnard*, 1995] producing a 51 km long lava flow (the longest on Hawai`i) [*Rowland and Walker*, 1990], covering an area of 91 km$^2$, burying the village of Wainānāli`i, and producing 383 × 10^6 m^3 of lava [*Barnard*, 1995]. The 1877 submarine radial vent eruption in Kealakekua Bay began ten days after a short-lived summit phase (<1 day). The submarine eruption was also thought to have lasted <1 day [*Barnard*, 1995]. It was witnessed from land and by passengers aboard the steamer Kīlauea, who reported bubbling water, blocks of lava floating to the surface, and the smell of sulfur in the air [*Whitney*, 1877]. Several submersible programs have mapped portions of the submarine eruption, including the vent locations (at depths of 690 to 1,050 mbsl) and associated lava flows [*Normark et al.*, 1979; *Fornari et al.*, 1980; *Moore et al.*, 1985]. As shown below, the full extent of the flow field from this eruption is much larger than previously thought.

2.3. Radial Vent Formation Models

[7] Several ideas have been invoked to explain Mauna Loa's subaerial radial vents. *Stearns and Macdonald* [1946] originally identified these vents and proposed that they were part of a diffuse northern rift zone. Subsequent mapping has shown that the radial vents are non-parallel and too widely dispersed to define a rift zone [*Lockwood and Lipman*, 1987]. A recent gravity survey confirmed that Mauna Loa does not have a north rift zone [*Kauahikaua et al.*, 2000]. *Lockwood and Lipman* [1987] noted that ~20% of the subaerial radial vent eruptions lack near-vent structures (i.e., cones or spatter ramparts), indicating that the lava erupted had already degassed. This observation led to the suggestion that some radial vent eruptions resulted from leaky summit lava lakes [*Lockwood*, 1995]. This model, however, provides no explicit structural explanation for the formation of radial vent fractures. *Walker* [1990] offered a model for radial vent formation while attempting to rationalize the curvature of Hawaiian rift zones. He proposed that injection of a greater magma volume into the proximal versus distal portion of the rifts could create a bend in the once linear rift zones. This theory predicts the migration of Mauna Loa's upper rift and summit northwestward toward the two buttressing volcanoes (Mauna Kea and Hualālai) while the lower portions of the rift zones remain immobile. The bend in the rift zones would create extension on the northwestern flank of the volcano allowing for the formation of a third rift zone or radial vents [*Walker*, 1990]. Although it has been suggested that the lower portion of Mauna Loa's southwest rift zone has migrated westward [*Lipman*, 1980], there is no evidence that the summit has shifted over time. *Rubin* [1990] proposed that radial dikes eruptions occur when the pressure in the rift zones becomes too high to allow injection of more magma. The absence of major faults or cracks in Mauna Loa's rift zones was used as evidence in support of this idea. The new strain meters that have recently been installed on Mauna Loa may allow this idea to be tested.

3. Seafloor Bathymetry and Geologic Map

3.1. Bathymetry Collection and Submersible Sampling

[8] A >300 km^2 area off the western coast of the island of Hawai'i (Figure 1) was selected for this study after our identification of cone-like features in previous bathymetry of the region [*Moore and Chadwick*, 1995]. Our 1999 dredging expedition sampled three of these possible cones in the Kealakekua Bay area [*Davis et al.*, 2003] and eight samples are included in this study. A new high-resolution bathymetric survey of Kealakekua Bay region was undertaken in October and November of 2002 using the Kongsberg Simrad EM300 high-resolution sonar system on the R/V *Thomas Thompson*. This 30-kHz multibeam system has up to 135 individual 1° (vertical) × 2° (horizontal) electronically formed beams. Technical specifications for this mapping system have been described by *Gardner and Hughes Clarke* [1998] and *Hughes Clarke et al.* [1996, 1998]. The system simultaneously collects bathymetry and coregistered backscatter data with navigation provided by Pcode GPS. Each depth determination is calculated using phase and amplitude detection and the net solution is selected on the basis of a set of statistical quality-control parameters. The vertical resolution of the EM300 is 0.2% of the water depth or <5 m for the Kealakekua Bay area [*Kongsberg Maritime*, 1997]. The Kealakekua Bay region was mapped at a ship speed of 8–10 knots.

[9] Photography and sampling of the Kealakekua Bay area using JASON2 was in integral part of our field program. We took advantage of the long dive time capability of this new ROV during four dives (J2-13, −14, −15, −18). JASON2 photographs for these dives are available at the Woods Hole Oceanographic Institution site http://www.whoi.edu/marops/vehicles/jason/van_cruises.html under Hawaii 2002, cruise tn151. Seventy one lavas were sampled from seven vents and other areas by JASON2.

3.2. Geologic Map

[10] Our bathymetry and acoustic backscatter maps (Figures 2 and 3) and derivative shaded relief map (Figure 4) can be used to identify a variety of geologic features on the western submarine flank of Mauna Loa, including volcanic cones and associated lava flows, lava fields with no identifiable connection to a volcanic cone, volcaniclastic and/or highly sedimented terrain, subaerially erupted lava flows, slump terraces, and landslide scars. Classification of a feature as a cone was based on the presence of at least one closed 20 m contour, relief >50 m (Figure 2), and slopes opposing the western dip of Mauna Loa's flank. Summit depressions (>10 m) were identified on four of the cones (Pa'ao, Mo'ikeha, Kahole-a-kane and Kua-o-wakea). The 1877 eruption flow field lacks a well

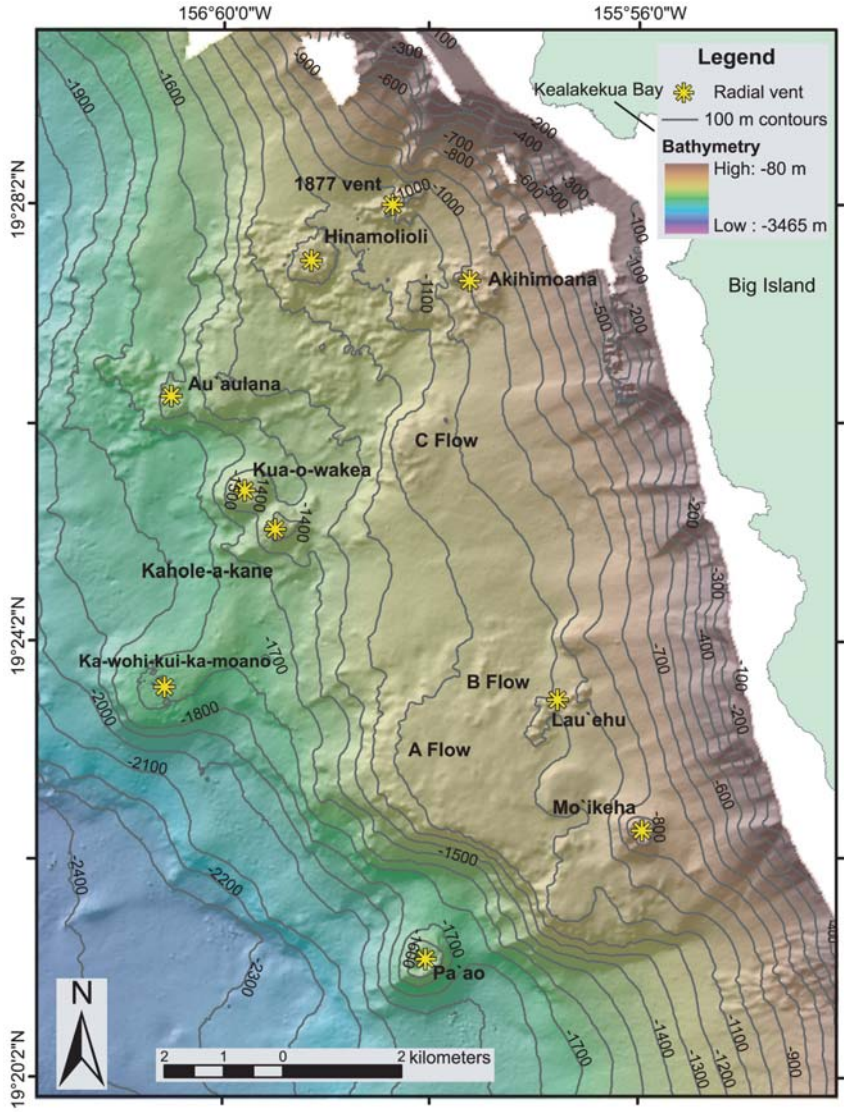

Figure 2. Bathymetry superimposed on a shaded relief image for Mauna Loa's western submarine flank near Kealakekua Bay. The locations of the 10 submarine radial vent cones are indicated by yellow asterisks. The contour interval is 100 m. Illumination for the shaded relief image is from the northwest. Processing of the data was done using MB-Systems [*Caress et al.*, 1996; *Guth et al.*, 1987; *Guth*, 2001] and GMT [*Wessel and Smith*, 1995]. Maps are projected in North American 1983 UTM zone 5 datum and have a spatial resolution of 25 m. ArcGIS software was used to produce this and other images of the study area.

defined cone, although we discovered a shallow depression with drainback features surrounded by spatter ramparts (Figure 5). Similar features were previously observed upslope in the shallower parts of the 1877 flow field and described as "primary vents and eruptive centers" [*Fornari et al.*, 1980]. On the basis of these criteria, there are ten submarine cones in the Kealakekua Bay area. All but the 1877 eruption were given Hawaiian names (Figure 2; Table 1) that tell of the ninth migration of sharks based on an oral tradition (P. Kanakaole-Kanahele, personal communication, 2005).

[11] The extents of Mauna Loa's submarine radial vent lava flows were determined using several data sets including backscatter imagery, bathymetry, shaded relief images, photography, and rock geochemistry (Table 1). Backscatter imagery was particularly useful in delineating the full extent of the 1877 eruption and in mapping its contacts with adjacent flows (Figure 3). Rock geochemistry was important in relating the distal portion of the lava flows to specific cones. The geochemical interpretations are supported by bathymetric data, backscatter images, and surface textures (Figures 2–4). Thus

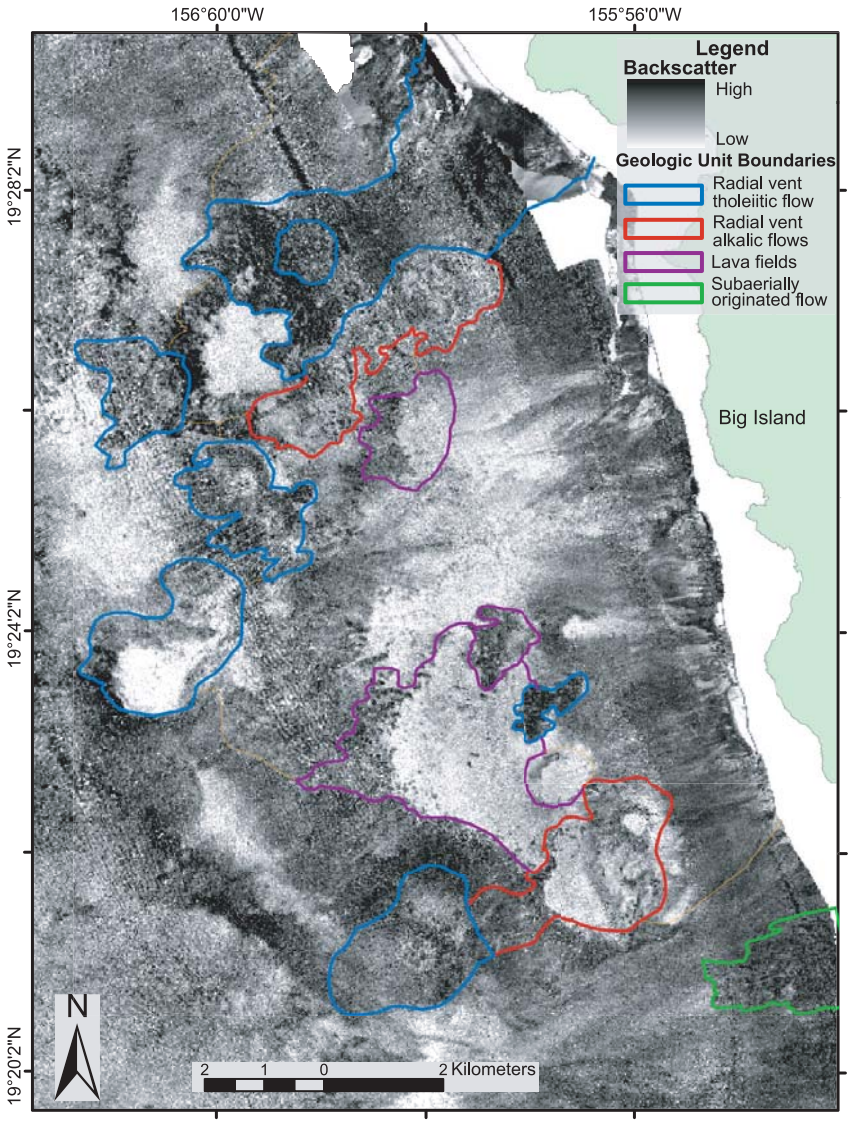

Figure 3. Acoustic backscatter image of Mauna Loa's western submarine flank near Kealakekua Bay overlain by outlines from the geologic map (Figure 5). Darkest colors represent areas of higher reflectivity (i.e., thinner sediment cover).

a highstanding lava flow (>10 m) that can be traced back to a cone in the bathymetry is considered to be related to that cone if the backscatter images support this interpretation. Seven of the vents produced flows >1 km in length, with the longest (4.2 km) originating from Akihimoana vent (Table 1).

[12] Surface texture from backscatter images and bathymetry are commonly used to distinguish submarine lava fields from the surrounding volcaniclastic slopes [e.g., *Moore and Chadwick*, 1995]. We were unable to link three flows to upslope cones, so they are not included with the submarine radial vent suite. These flows (A, B and C; Figure 6) could be related to subaerial lavas whose shallower portions have been buried by sediment or to radial vents that have no recognizable vent structures (>10 m high), as noted for 20% of subaerial Mauna Loa radial vents [*Lockwood and Lipman*, 1987]. Flow C (~1.5 km^2), in the central part of the map area, was photographed and sampled. The two other southern flows (A and B) were identified only from bathymetry and backscatter images (Figures 2 and 3). Flow A covers ~5.1 km^2; flow B is much smaller (~0.7 km^2) and is highly reflective in backscatter images, suggesting it is young. The submarine extension of one subaerially erupted lava flow was identified in the study area

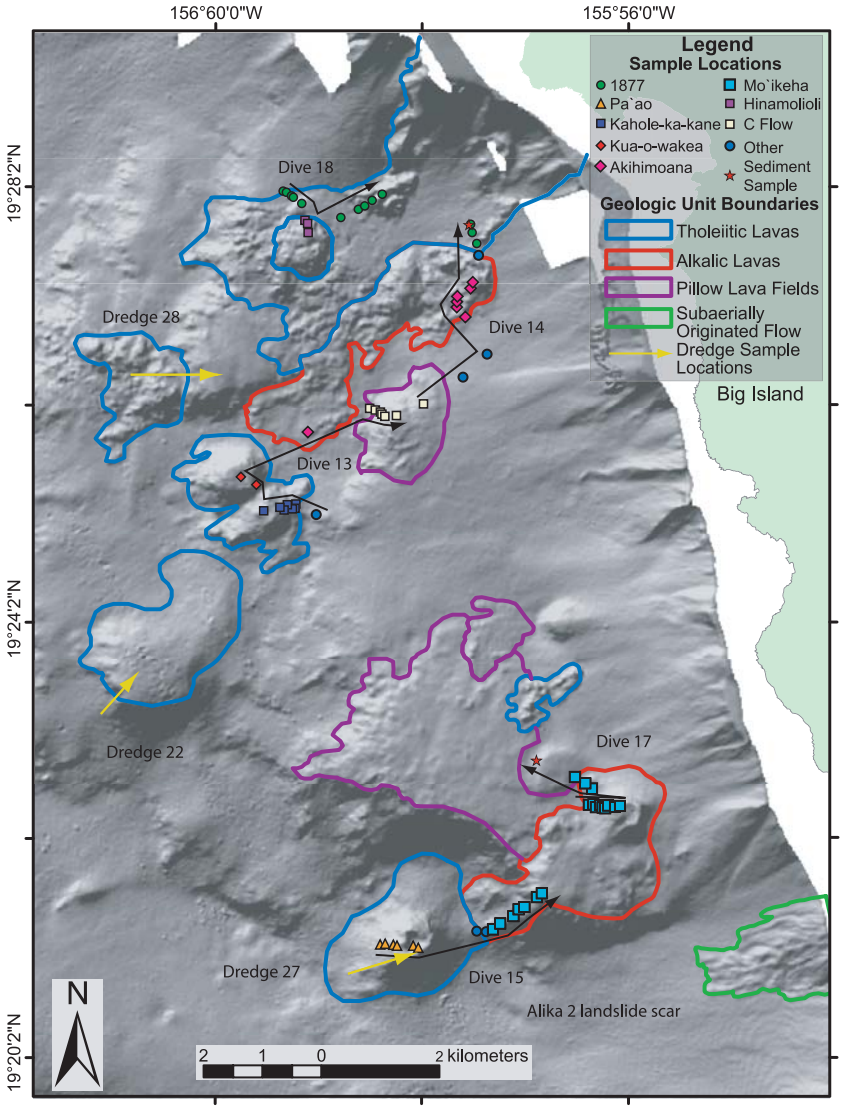

Figure 4. Shaded relief image of Mauna Loa's western submarine flank near Kealakekua Bay with illumination from the northwest. The locations of samples collected by JASON2 are shown with different symbols for each radial vent. Black lines indicate the direction of the dive lines. The locations of dredges taken in 1999 are shown with red lines.

(Figure 3). The subaerial flow, Waiea, is considered to be relatively young (750–1500 years B.P.) [*Wolfe and Morris*, 1996]. It overlies the Alika 2 landslide scar [*Moore and Chadwick*, 1995] at the southern end of the study site (Figure 2) and reaches a maximum height of ~50 m. It was not sampled during this study.

[13] Mauna Loa's western, nearshore submarine flank is characterized by relatively smooth textures (Figure 2). This area is thought to be covered by epiclastic sediment or volcaniclastics produced by fragmentation of subaerially erupted lava entering the ocean [*Moore and Fiske*, 1969; *Moore and Chadwick*, 1995]. Sediment samples taken ~3.5 and 5.5 km offshore consist of a mixture of fine-grained carbonate sand, siliceous spicules, and basaltic glass chips (up to 2 cm in size) in a muddy matrix. A thin layer of similar material was seen on top on most radial vent pillow lavas. Backscatter imagery (Figure 3) indicates that the nearshore slope is streaked with sediment debris channels, which has been attributed to tidal swashing as fine fractions are winnowed from coarser sediments [*Fornari and Campbell*, 1987].

[14] The Kealakekua Bay area contains three broad, sediment-covered terraces, which may be

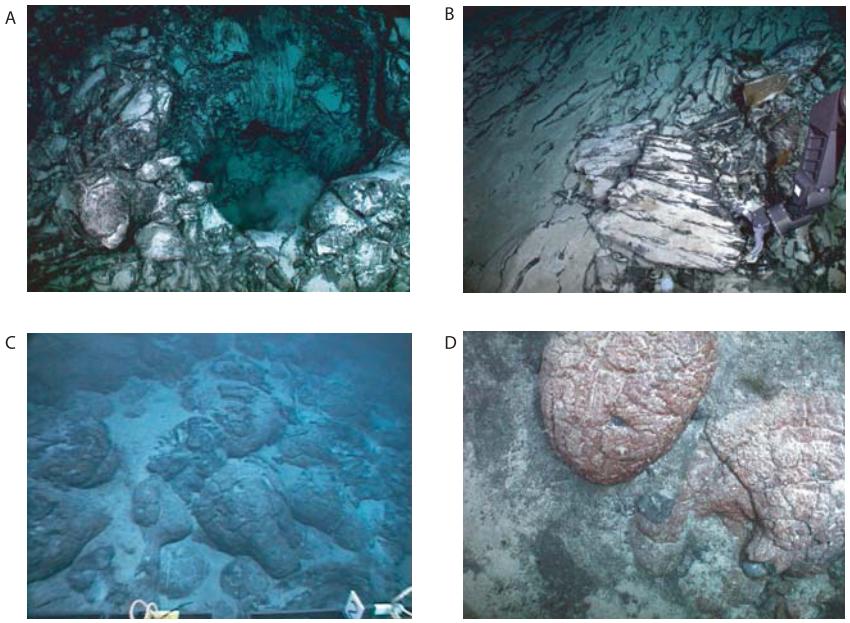

Figure 5. Outcrop photos of lava flows taken by JASON2 video cameras. (a) Submarine vent from the 1877 flow. Drainback features are visible on the northern rim of the vent. The depression is surrounded by loose spatter like fragments. (b) Large, glassy sheet flow from the 1877 eruption. It is covered with a thin layer of sediment and is located ~1.5 km from the vent. (c) Mound of pillow lavas on the flanks of Pa'ao cone. Sediment fills gaps between bulbous pillows. (d) Two bulbous pillow lavas with red, striated surface erupted from Kahole-a-kane vent.

related to the North Kona slump [*Moore and Chadwick*, 1995]. The last major movement of this slump is thought to have occurred prior to 130 ka [*Moore and Clague*, 1992]. Nine of the radial vents were built on these terraces. The southern portion of this region is cut by the Alika 2 landslide [*Moore and Chadwick*, 1995]. The age of Alika 2 landslide has been estimated at 112 ± 15 to 127 ± 5 ka [*McMurtry et al.*, 1999]. The Pa'ao vent erupted within the Alika 2 landslide scar (Figure 4).

[15] On the basis of the analyses and interpretations from these different data sets, we have produced a detailed geologic map of the Kealakekua Bay study site (Figure 6). This is the first map of a Hawaiian submarine area that delineates individual lava flows and vents.

3.3. Eruption Volumes

[16] The volume of each submarine radial vent eruption was estimated from gridded multibeam data using ArcGIS. We measured the depths of the flow and surrounding seafloor at 5–10 locations for each flow to determine the average flow thickness. The area of each flow was calculated using the geologic map. On the basis of our previous ArcGIS work, we estimate the uncertainties in volume estimates as ±10%. A horizontal plane was placed through the average base height of each cone and estimating the volume of material above the plane for each eruption. This approach worked well for the cones and lava flows erupted on low-angled slopes (i.e., Kahole-a-kane or Pa'ao; Figure 2). However, volumes for flows that traveled over a slope of >10° (i.e., Mo'ikeha, Akihimoana, and 1877) were calculated in multiple steps. Volumes for Kahole-a-kane and Kua-o-wakea, two adjacent cones (Figure 2), were combined because these cones produced petrographically and geochemically identical lavas (see below). The volumes for the submarine radial vent eruptions vary by more than an order of magnitude (10 to 430 × 10^6 m^3 ± 10%; Table 1), as observed for subaerial radial vent flows [*Lockwood and Lipman*, 1987].

4. Petrology

4.1. Outcrops and Samples

[17] The submarine Mauna Loa lavas consist primarily of striated bulbous and elongate pillows, although a sheet flow was discovered in the 1877 flow field (Figure 5), and spatter-like ramparts were found at one of its vents at ~900 m below sea level. The submarine radial vent sample suite

Table 1. Physical Characteristics of Mauna Loa's Radial Vent Cones and Flows

Feature	1877	Laʻehu	Paʻao	Kahole-a-kane	Kua-o-wakea	Akihimoana	Moʻikeha	Auʻaulana	Hinamolioli	Ka-wohi-kui-ka-moana	C Flow	B Flow	A Flow
Elevation, mbsl[a]	990	960	1560	1375	1400	1080	800	1540	1160	1640	1110	1145	1120
Cone h,[g] m	110	65	375	230	260	150	230	190	100	200			
Base diameter, m	620	440	1600	800	1050	960	1000	1100	700	2100			
Top diameter, m	310	190	400	380	425	500	400	500	580	1200			
Aspect ratio, h/basal diameter	0.18	0.15	0.23	0.29	0.25	0.16	0.23	0.17	0.14	0.10			
Flatness ratio[b]	0.50	0.43	0.25	0.48	0.40	0.52	0.40	0.45	0.83	0.57			
Approximate flow thickness, m	10	10	20	25	20	20	80	25	–	–	10	10	15
Flow length, km	3.6	0.8	1.5	1.1	0.6	4.2	2.8	1.7	0	1.5			
Area, km^2	7.0	0.2	0.3	1.2	1.1	3.8	1.6	1.6	0.7	3.8	1.5	0.7	5.1
GIS total volumes, $\times 10^6$ m^3	434	10	331	211[c]		400	163	100	29	344	60	5	206
Vol comparison,[d] $\times 10^6$ m^3	112[e]	5	330	183[c]		113[e]	94	99	31	330			
Sediment cover[f]	1	na	3	3.5	3	4	5	na	5	na	4	na	na
Acoustic reflectivity	high	high	medium	medium	medium	medium	low	medium	low	low	low	low	high
Mn thickness, mm	0	na	0.029	0.029	na	0.039	0.049	0.078	0.078	0.118	0.049	na	na
Estimated age from Mn-coating, ka	0	na	12	12	na	16	20	31	31	47	20	na	na
Composition	Thol	?	Thol	Thol	Thol	Alk	Alk	Thol	Thol	Thol	Thol	?	?

[a] Elevation (mbsl) equals the shallowest point of cone.
[b] Flatness ratio = summit diameter/ basal diameter.
[c] Volume estimates were combined due to the fact that geochemical, physical, and spatial evidence indicates that they were produced during the same eruption.
[d] Approximate cone Vol (m^3) was calculated using the equation for a truncated cone except where indicated flow volumes are not included in this calculation.
[e] Approximate cone Vol (m^3) were calculated for entire flow and cone using the equation surface area x flow height.
[f] 1 is thinnest sediment cover; 5 is thickest sediment cover.
[g] h, height.

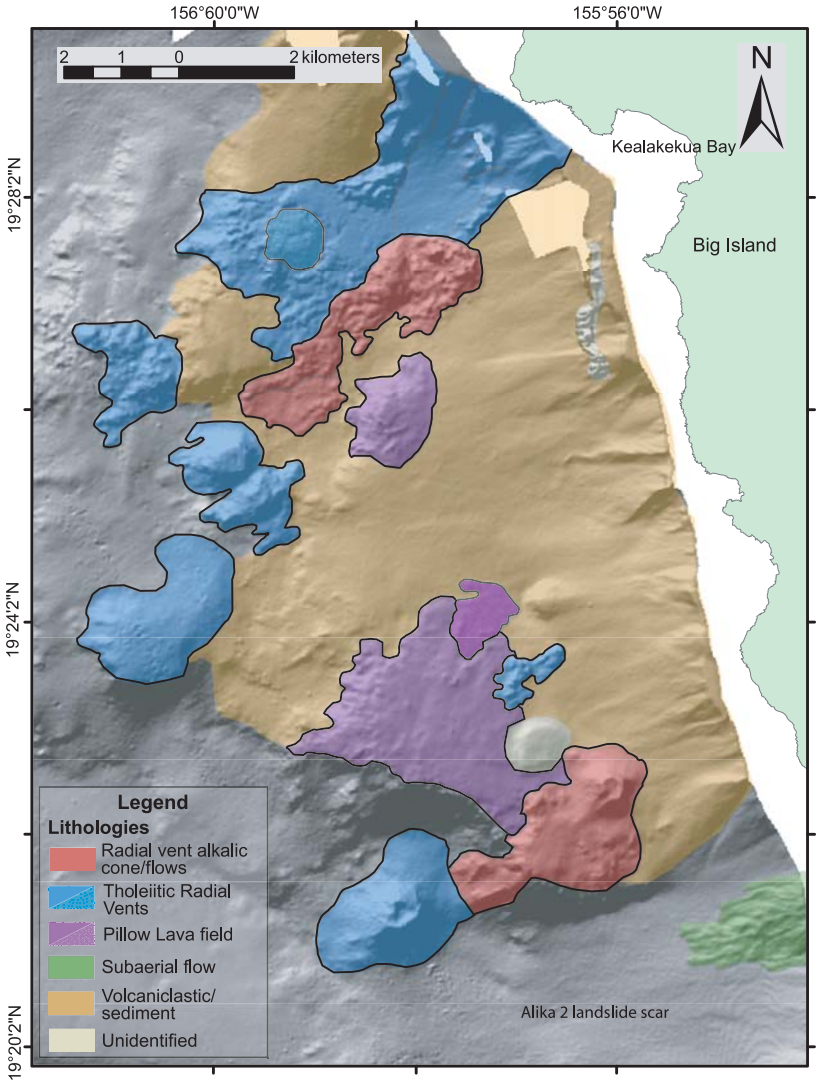

Figure 6. Geologic map of Mauna Loa's western submarine flank near Kealakekua Bay. Stippled patterns are used to distinguish between two adjacent flows of a similar rock type. The west coast of the island of Hawai`i is shown in pale green. White regions were not surveyed. See text for details on how map was produced and legend for rock types.

includes 71 lavas collected using JASON2 (labeled with a J2 prefix followed by a dive number in Tables 2–5) and eight rocks dredged from three vents in 1999 (all labeled with an M prefix followed by dredgehaul number). The suite includes 67 samples collected from the radial vent cones and their associated lava flows, seven from the C flow, and five from other flows of unknown origin. Four of these five lava samples were collected between cones and have distinct compositions. The lavas range in color from black to red and have thin (<1 cm) glassy rims. One unusual sample (13-01) has high vesicularity (~29%) and modal olivine (~17%) and was not collected in situ. Thus it is probably a subaerial lava that rolled down slope and is not displayed in the geochemistry plots.

4.2. Petrography

[18] Modes on 48 Mauna Loa radial vent and eight C flow samples show that they are mostly aphyric (<1 vol.%), weakly vesicular (average ~ 1.7 vol.%) basalts (Table 2), which is atypical for Mauna Loa submarine lavas. Among phenocrysts (width $\geq$ 0.5 mm), olivine is the most common (~0.4 vol.%), followed by plagioclase (~0.2 vol.%) and rare clinopyroxene (cpx; ~0.1 vol.%). Microphenocrysts (width 0.1–0.5 mm) are more abundant (olivine - 1.9 vol.%, plagioclase - 3.3 vol.%, and

Table 2. Petrography of Mauna Loa's Submarine Radial Vents and Other Submarine Lavas[a]

		Olivine		Plag		Cpx		Opx		Opaq		
Vent	Sample	ph	mph	ph	mph	ph	mph	ph	mph	mph	Matrix	Ves
South 1877	J2-14-11	<0.1	2.0	0.0	0.2	<0.1	1.2	0.0	<0.1	0.2	96.4	8.0
	J2-14-14	<0.1	1.2	0.6	0.4	0.0	0.4	0.0	<0.1	<0.1	97.4	8.8
	J2-14-12	<0.1	0.4	0.0	0.2	<0.1	0.6	0.0	<0.1	<0.1	98.8	7.8
North 1877	J2-18-12	0.8	0.2	0.0	0.4	<0.1	3.8	0.0	<0.1	<0.1	94.8	4.6
	J2-18-01	1.6	3.2	<0.1	1.4	0.2	1.6	0.0	0.2	<0.1	91.8	0.2
	J2-18-05	0.6	1.0	<0.1	2.4	<0.1	2.4	0.0	0.4	<0.1	93.2	<0.1
	J2-18-10	0.8	0.8	0.0	1.8	0.0	2.0	0.0	1.2	<0.1	93.4	1.6
	J2-18-11	0.2	2.0	<0.1	1.6	<0.1	0.8	0.0	1.2	<0.1	94.2	3.0
	J2-18-13	0.4	1.0	0.2	0.6	<0.1	2.2	<0.1	0.8	<0.1	94.8	6.0
	J2-18-04	1.8	1.2	0.4	2.6	<0.1	1.2	0.0	0.4	<0.1	92.4	0.0
	J2-18-03	0.6	1.2	<0.1	1.0	<0.1	1.2	0.0	0.6	<0.1	95.4	1.0
	J2-18-02	0.2	1.4	0.2	3.0	0.0	2.2	0.0	0.4	<0.1	92.6	0.2
Pa'ao	J2-15-06	0.4	0.6	1.0	2.2	0.4	3.4	0.0	0.0	0.0	92.0	0.2
	J2-15-03	0.2	1.2	0.2	4.2	1.2	2.8	0.0	0.0	<0.1	90.2	0.8
	J2-15-05	0.2	0.6	0.2	3.8	0.0	5.2	0.0	0.0	<0.1	90.0	0.4
	J2-15-04	0.0	1.2	0.6	7.0	0.4	3.8	0.0	0.0	<0.1	87.0	0.6
	J2-15-01	0.2	1.0	0.6	3.0	0.6	2.6	0.0	0.0	0.0	92.0	0.2
	J2-15-02	0.0	0.8	1.0	3.0	0.8	4.4	0.0	0.0	0.0	90.0	0.1
	M27-2[b]	0.4	0.8	0.6	3.4	0.4	3.2	0.0	0.0	0.0	91.2	<0.1
	M27-11[b]	0.4	2.0	0.6	4.8	1.4	5.8	0.0	0.0	0.0	85.0	<0.1
Kahole-a-kane	J2-13-02	0.2	1.2	<0.1	5.6	0.2	1.8	0.0	0.0	<0.1	91.0	1.2
	J2-13-05B	0.6	1.0	<0.1	4.8	0.0	1.0	0.0	0.0	<0.1	92.6	<0.1
	J2-13-04B	<0.1	1.4	0.2	5.6	0.0	1.0	0.0	0.0	0.0	91.8	<0.1
	J2-13-06	0.4	5.8	0.4	4.4	0.0	2.0	0.0	0.0	0.0	87.0	0.2
	J2-13-04A	0.2	1.2	<0.1	10.4	0.4	1.8	0.0	0.0	0.0	86.0	<0.1
	J2-13-05A	1.0	0.8	0.4	7.0	0.0	0.8	0.0	0.0	0.0	90.0	1.2
	J2-13-03	<0.1	1.4	0.2	5.6	0.2	1.6	0.0	0.0	0.0	91.0	<0.1
Kua-o-wakea	J2-13-07	0.2	5.6	<0.1	6.6	0.2	1.6	0.0	0.0	<0.1	85.8	<0.1
	J2-13-08	<0.1	3.5	0.4	2.6	0.4	2.0	0.0	0.0	<0.1	91.1	1.0
Hinamolioli	J2-18-07	0.0	1.7	0.0	1.4	0.0	2.8	0.0	0.0	0.0	94.1	0.2
	J2-18-08	0.0	0.6	0.0	2.0	0.0	1.6	0.0	0.0	0.0	95.8	0.2
	J2-18-06	0.0	1.0	0.0	2.8	0.0	3.0	0.0	0.0	0.0	93.2	0.4
Ka-whohi-kui-ka-moana	M22-11[b]	24.2	2.2	0.0	0.4	0.8	0.2	0.0	0.0	0.0	72.2	0.6
	M22-4[b]	23.0	3.8	0.0	0.6	0.0	0.2	0.0	0.0	0.0	72.4	<0.1
C Flow	J2-13-12	1.0	1.8	<0.1	3.2	0.0	1.6	0.0	0.0	<0.1	92.4	<0.1
	J2-13-14	2.2	5.6	<0.1	2.2	0.0	0.8	0.0	0.0	<0.1	89.2	1.0
	J2-13-13	1.6	1.8	<0.1	0.8	0.0	0.0	0.0	0.0	<0.1	95.8	<0.1
	J2-13-15	<0.1	4.6	<0.1	10.4	0.0	2.4	0.0	0.0	<0.1	82.6	0.8
	J2-13-11	1.4	6.2	<0.1	1.4	0.0	0.6	0.0	0.0	<0.1	90.4	0.2
	J2-13-16	0.2	4.8	<0.1	13.2	0.0	7.0	0.0	0.0	0.4	74.8	0.2
	J2-13-09	0.6	4.6	0.2	3.6	0.0	1.8	0.0	0.0	0.0	89.2	0.6
	J2-14-01	1.2	2.2	0.0	2.6	0.0	1.2	0.0	0.0	0.2	92.8	1.4
Other flows	J2-14-03	<0.1	0.4	0.0	0.4	0.0	0.2	<0.1	0.4	0.4	98.6	<0.1
	J2-14-02	0.8	0.2	0.0	0.4	0.0	0.4	0.0	0.0	<0.1	98.2	2.4
	J2-14-10	0.2	3.0	0.4	4.6	0.0	0.0	0.0	0.0	<0.1	91.8	0.6
	J2-15-07	2.0	0.4	1.8	3.2	0.6	3.6	0.0	0.0	<0.1	88.4	<0.1
	J2-15-08	3.8	1.4	0.2	4.0	0.2	2.4	0.0	0.0	<0.1	88.0	<0.1
	J2-13-01[c]	17.4	0.2	0.4	4.4	0.8	0.2	0.0	0.0	0.2	76.6	29.4

[a] In vol%. Based on 500 pt count modes; samples listed in order of whole rock MgO content; matrix is vesicle-free.
[b] Dredge samples (data from *Davis et al.* [2003]); all other modes by A. Miller.
[c] Sample not taken in place.

cpx - 2.0 vol.%). Orthopyroxene (opx) was found in lavas from only one vent (1877), where it occurs as rare microphenocrysts (~0.6 vol.%). It is mantled by a thin cpx rim, a previously recognized distinctive texture of lavas from this eruption [*Moore et al.*, 1985]. Samples from the south arm of the 1877 flow contain fewer phenocrysts and microphenocrysts, and are more vesicular than samples from the north arm (Table 2). Lavas from two other vents are distinctive; Pa'ao lavas

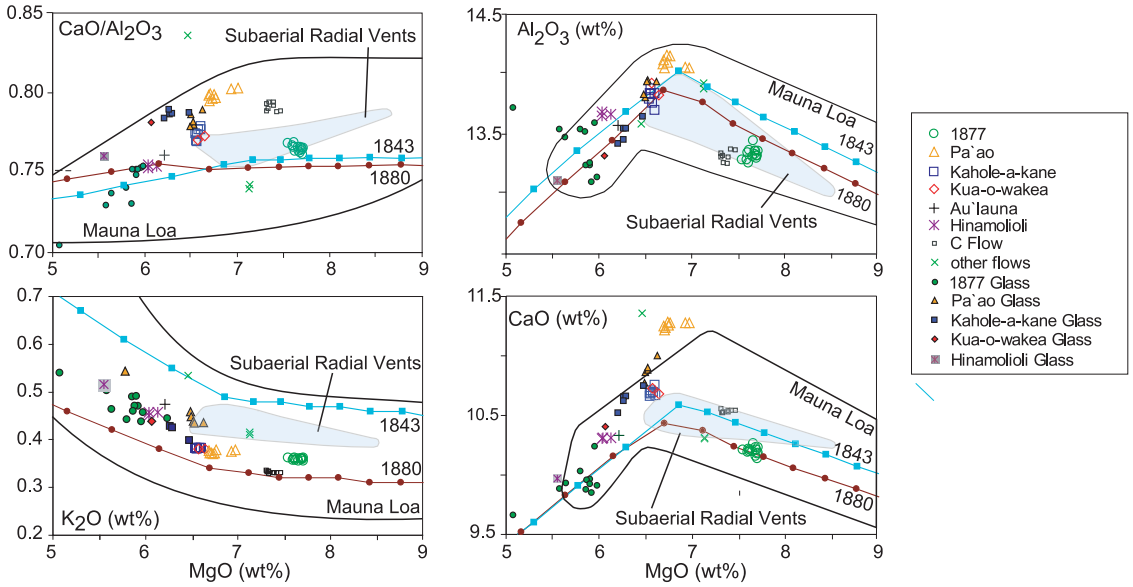

Figure 7. MgO variation diagrams for CaO, Al_2O_3, K_2O, and CaO/Al_2O_3 for Mauna Loa's submarine tholeiitic lavas. The field for the subaerial radial vents is shown in blue. The thick black line represents the field for Mauna Loa lavas (whole rock data). Whole rock data are represented by open symbols, whereas corresponding glass data for each flow are shown as shaded symbols. The 1 atmosphere liquid lines of descent (calculated using MELTS) [*Ghiorso and Sack*, 1995] for two possible Mauna Loa compositional end-members (1843 and 1880 eruption lavas) [*Rhodes and Hart*, 1995] are shown for comparison. The modeling conditions were fractional crystallization in 1°C steps, low amounts of water (0.16 wt.%) to accommodate the degassed nature of most of the radial vent lavas, low pressure (1 bar), and the Quartz Fayalite Magnetite (QFM) oxygen fugacity buffer. Many radial vent samples do not plot along these liquid lines of descent and must have distinct parental magmas. Data for Mauna Loa fields are from *Rhodes* [1995], *Rhodes and Hart* [1995], *Rhodes and Vollinger* [2004], and J. M. Rhodes (unpublished data). Analytical error is smaller than the symbol size.

contain more cpx (3–5%) and Ka-wohi-kui-ka-moana lavas have much higher olivine abundances (23–24 vol.%). High olivine abundances are common among Mauna Loa's submarine southwest rift [*Garcia et al.*, 1989, 1995]. Overall, lavas from each vent are petrographically similar (Table 2), although minor differences probably reflect variations in crystallinity and segregation of minerals during flow.

[19] Thin coatings of manganese-iron (Mn-Fe) were found on some Mauna Loa submarine lavas. They range in thickness from 0.029 to 0.118 mm (Table 1). The error estimate (±0.001 mm) reflects repeated measurements of the maximum thickness on each sample by two observers. Ka-wohi-kui-ka-moana lavas have the thickest Mn-Fe coating, whereas no coating was observed on the 1877 lavas. A thin palagonite layer (≤0.39 mm thick) occurs beneath most of the Mn-Fe coatings.

4.3. Glass Compositions

[20] Major element and S analyses were obtained by microprobe on 44 tholeiitic submarine radial vent glasses at the University of Hawai'i following methods described by *Garcia et al.* [1995]. Geochemical data for the alkalic samples are presented by *Wanless et al.* [2006]. The glass analyses are an average of five spot analyses per sample. Accuracy and precision are estimated at <1% for major elements and 2–5% for minor elements based on repeat analyses of a Hawaiian glass standard (A99). The composition of these submarine glasses is typical of Mauna Loa glasses (Figure 7), including their relatively high silica content (50.8 to 52.9 wt%; Table 3) [e.g., *Garcia*, 1996]. Glass MgO contents are relatively low (6.5 to 5.1 wt%) indicative of eruption temperatures of 1,129 to 1,162°C, based on the MgO geothermometer (temperature °C = 23 × MgO wt% + 1012) of *Montierth et al.* [1995]. Several of the glasses have lower Al_2O_3 (13.2–13.9 wt%) and CaO (9.7–11.0 wt%) than their respective whole rock compositions (Figure 7). These lower values are consistent with petrography for these lavas, which indicate crystallization of plagioclase and cpx. Glass CaO/Al_2O_3 ratios generally show little or no variation (Figure 7) indicating consistent proportions of plagioclase

Table 3. Microprobe Glass Analyses of Mauna Loa's Submarine Radial Vent and Other Submarine Lavas

Vent	Label	SiO_2	TiO_2	Al_2O_3	FeO	MnO	MgO	CaO	Na_2O	K_2O	P_2O_5	S	Total
South 1877	J2-14-11	51.53	2.85	13.72	12.93	0.16	5.08	9.66	2.52	0.54	0.26	0.135	99.39
	J2-14-14	51.85	2.47	13.84	11.81	0.16	6.24	10.33	2.41	0.45	0.23	0.117	99.89
	J2-14-12	51.51	2.65	13.52	12.63	0.18	5.86	9.88	2.48	0.49	0.23	0.124	99.56
North 1877	J2-18-12	52.19	2.49	13.24	12.90	0.18	5.87	9.95	2.53	0.46	0.23	0.127	100.16
	J2-18-01	52.92	2.59	13.54	12.07	0.19	5.58	9.88	2.59	0.50	0.25	0.075	100.18
	J2-18-05	52.10	2.51	13.54	12.02	0.18	5.80	10.03	2.38	0.44	0.26	0.083	99.35
	J2-18-10	51.97	2.51	13.10	12.88	0.20	5.92	9.85	2.53	0.47	0.25	0.139	99.83
	J2-18-11	52.06	2.52	13.14	12.75	0.19	5.98	9.91	2.58	0.46	0.25	0.135	99.99
	J2-18-09	52.11	2.43	13.60	11.85	0.16	5.96	10.24	2.40	0.44	0.28	0.134	99.59
	J2-18-13	52.34	2.40	13.26	12.80	0.21	5.90	9.92	2.56	0.47	0.23	0.132	100.22
	J2-18-04	52.54	2.55	13.24	12.58	0.18	5.90	9.96	2.47	0.49	0.24	0.075	100.24
	J2-18-02	52.18	2.59	13.47	12.13	0.19	5.64	9.93	2.42	0.46	0.28	0.069	99.38
Pa'ao	J2-15-06	51.04	2.58	13.94	11.86	0.18	6.52	10.90	2.47	0.44	0.22	0.023	100.17
	J2-15-03	50.97	2.47	13.94	11.98	0.17	6.62	11.00	2.44	0.43	0.23	0.016	100.27
	J2-15-05	50.84	2.52	13.83	12.19	0.17	6.49	10.78	2.47	0.46	0.24	0.022	100.00
	J2-15-01	50.96	2.54	13.81	12.22	0.19	6.50	10.86	2.47	0.45	0.23	0.013	100.23
	J2-15-02	51.01	2.49	13.95	11.99	0.17	6.53	10.88	2.46	0.44	0.26	0.030	100.20
	M27-01[a]	51.59	2.32	13.75	10.83	0.20	6.37	10.61	2.38	0.46	0.29	0.009	98.81
	M27-02[a]	51.57	2.48	13.48	11.51	0.21	6.29	10.85	2.37	0.43	0.26	0.014	99.46
	M27-11[a]	51.60	2.45	13.40	11.54	0.17	6.25	10.75	2.41	0.44	0.28	0.013	99.30
	M27-12[a]	51.50	2.49	13.49	11.91	0.16	6.29	10.85	2.43	0.43	0.30	0.014	99.86
	M27-28[a]	52.38	2.47	13.55	10.26	0.14	6.31	10.82	2.40	0.40	0.30	0.009	99.04
	M27-37[a]	52.76	2.21	13.76	10.39	0.19	6.49	10.61	2.46	0.44	0.23	0.006	99.55
Kahole-a-kane	J2-13-02	52.09	2.40	13.55	12.03	0.19	6.27	10.65	2.34	0.43	0.23	0.016	100.18
	J2-13-05B	51.60	2.39	13.46	12.04	0.19	6.26	10.62	2.37	0.43	0.22	0.013	99.59
	J2-13-06	51.71	2.41	13.42	12.13	0.18	6.21	10.52	2.36	0.43	0.23	0.012	99.60
	J2-13-03	52.10	2.39	13.55	11.99	0.18	6.29	10.66	2.35	0.43	0.24	0.014	100.19
Kua-o-wakea	J2-13-07	51.72	2.52	13.32	12.32	0.19	6.06	10.41	2.42	0.44	0.23	0.016	99.64
	J2-13-08	52.21	2.50	13.51	12.16	0.18	6.20	10.49	2.27	0.40	0.21	0.010	100.13
Au'aulana	M28-01[a]	52.15	2.65	13.02	12.83	0.19	5.50	9.97	2.50	0.50	0.30	0.014	99.62
	M28-10[a]	51.66	2.70	12.77	12.90	0.21	5.29	9.84	2.57	0.53	0.32	0.013	98.80
	M28-11[a]	52.29	2.67	12.97	12.87	0.22	5.54	9.91	2.47	0.53	0.30	0.013	99.78
	M28-14[a]	52.19	2.66	13.00	12.91	0.19	5.54	9.94	2.46	0.54	0.30	0.014	99.74
	M28-21[a]	52.16	2.36	13.63	10.17	0.22	6.62	10.99	2.38	0.40	0.28	0.016	99.23
Hinamolioli	J2-18-06	51.67	2.72	13.11	13.01	0.20	5.55	9.97	2.49	0.52	0.32	0.011	99.56
Ka-wohi-kui-ka-moano	M22-04[a]	52.69	2.37	14.06	9.94	0.18	6.79	10.77	2.37	0.39	0.23	0.011	99.80
	M22-11[a]	52.11	2.49	13.74	10.51	0.18	6.33	10.62	2.48	0.40	0.27	0.011	99.14
C Flow	J2-13-14	51.02	2.38	13.59	11.91	0.17	6.48	11.02	2.39	0.42	0.22	0.019	99.62
	J2-13-15	50.89	2.49	13.57	11.95	0.20	6.43	10.95	2.41	0.44	0.23	0.026	99.58
	J2-13-11	50.80	2.64	13.54	12.17	0.18	6.29	10.83	2.41	0.42	0.22	0.023	99.52
	J2-13-09	51.96	2.56	13.41	12.10	0.18	6.15	10.46	2.33	0.39	0.20	0.014	99.75
Other flows	J2-15-07	52.12	3.00	13.45	12.38	0.17	5.78	9.87	2.60	0.54	0.29	0.018	100.22
	J2-15-08	51.94	3.06	13.38	12.79	0.19	5.49	9.75	2.65	0.57	0.30	0.018	100.13
	J2-13-01[b]	52.45	2.46	13.65	11.35	0.17	6.48	10.75	2.34	0.40	0.20	0.008	100.24

[a] Dredge samples (data from *Davis et al.* [2003]).
[b] Sample not collected in place.

and clinopyroxene crystallization. Most of the glasses have low sulfur values (0.01 to 0.03 wt%; Figure 8), typical of subaerial Mauna Loa lavas [e.g., *Davis et al.*, 2003]. Glasses from the 1877 eruption are distinct in having low CaO/Al_2O_3 and high S concentrations (0.07 to 0.14 wt%). The 1877 samples with slightly lower S (0.07–0.08 versus 0.11–0.14 wt%) were collected further from their vent indicating minor degassing during flowage, despite the ~1 km depth of the vent (Figure 2). The alkalic glasses from Akihimoana are also S-rich, although they have higher FeO contents similar to the S-poor glasses from the C flow (Figure 8).

4.4. Whole Rock XRF Data

[21] XRF major and trace element analyses were made on 53 tholeiitic submarine radial vent lava samples (Table 4; see also auxiliary material[1] Table S1) at the University of Massachusetts following

[1] Auxiliary material is available at ftp://ftp.agu.org/apend/gc/2005gc001086.

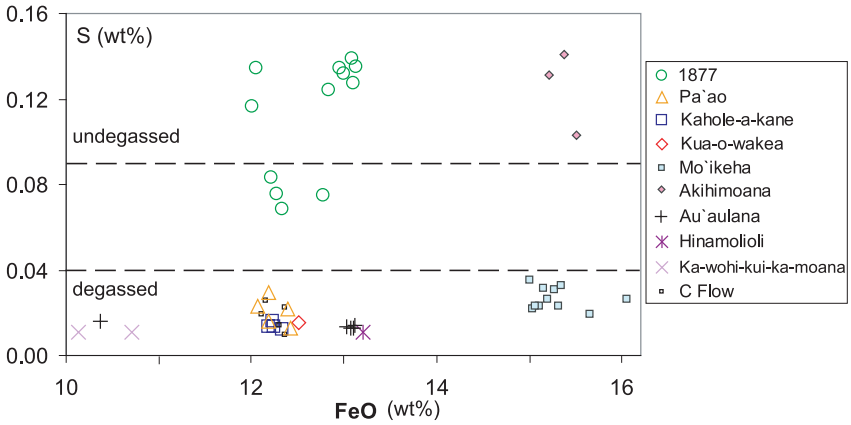

Figure 8. Total iron (as FeO) versus S in glasses from Mauna Loa's submarine lavas. Dashed lines separate undegassed glasses from partially and strongly degassed glasses, as defined by *Moore and Clague* [1987] and *Davis et al.* [2003]. Most of the radial vent lavas have degassed signatures (<0.04 wt%), similar to subaerially erupted Mauna Loa lavas [*Davis et al.*, 2003], despite being erupted at water depths sufficient to inhibit degassing (≥1000 m) [*Moore and Fabbi*, 1971]. The 1877 glasses show partially degassed to undegassed signatures (0.04 to >0.09 wt%). Akihimoana alkalic glasses are also degassed. Analytical error is <5% at 1000 ppm S to ~10% at 200 ppm S, and the symbol size for FeO.

methods described by *Rhodes and Vollinger* [2004]. The weakly phyric nature of most of these rocks (<2 vol.% phenocrysts; Table 2) suggests that the whole rock compositions are indicative of liquid compositions. All of the tholeiitic submarine lavas have major element compositions comparable to subaerial Mauna Loa lavas (Figure 7). Most of the submarine radial vent lavas, however, plot outside of the field for subaerial radial vent lavas in whole rock major element compositions (Figure 6). Multiple samples from individual vents and the C flow field cluster together and in many cases are distinct in composition compared to lavas from other vents. Kahole-a-kane and Kua-o-wakea (two adjacent cones) are an exception, with essentially identical compositions (Figure 7). Most of the submarine radial vent lavas have relatively low MgO (<8 wt%), and a lower K_2O for a given MgO compared to radial vent lavas (Figure 7). Lavas from Ka-wohi-kui-ka-moana have much higher MgO values (15–18 wt%) than other submarine lavas but plot within the subaerial Mauna Loa field [e.g., *Rhodes*, 1995; *Rhodes and Hart*, 1995]. These higher MgO values are consistent with their high modal olivine (23–24 vol.%; Table 2). Whole rock CaO/Al_2O_3 ratios for the submarine lavas range from 0.71 to 0.84, with the lowest ratios in the most fractionated lavas (Figure 7). The least fractionated lavas have CaO/Al_2O_3 ratios of 0.74 to 0.80 indicating a range of parental magma compositions.

[22] The submarine tholeiitic lavas have XRF-determined compatible and incompatible trace element abundances similar to other Mauna Loa lavas, including subaerial radial vent lavas (Figure 9). However, some of these submarine lavas have higher or lower Cr concentrations at a given K value compared with the subaerial radial vent lavas (Figure 9). The Hinamolioli and Auraulana lavas plot toward the lower part of the Mauna Loa field in the Sr plot (Figure 9), which is consistent with petrographic and major element evidence for plagioclase fractionation in these lavas (Figure 7). The C flow has slightly higher Nb and Sr contents for a given K concentration compared to the subaerial radial vent samples (Figure 9).

4.5. ICPMS Data

[23] ICPMS analyses were done on 15 tholeiitic submarine lavas (Table 5) at the Australian National University following methods described by *Norman et al.* [1998]. These submarine lavas, like other Mauna Loa lavas, have light REE-enriched patterns (Figure 10). Although samples with lower MgO tend to have higher REE concentrations (Tables 4 and 5), the mild fanning and crossing REE patterns (Figure 10) cannot be explained by low pressure fractionation of the observed minerals in these rocks (Table 2). The sample with the highest light REE content and steepest pattern (J2-14-10) is the most alkaline (alkalinity −0.87 versus −1.7 to −3.6 ± 0.2 for the other samples; Figure 10). Fanning patterns and variable alkalinity in Hawaiian lavas have been explained by variable degrees of partial melting of a garnet-bearing source [e.g., *Lanphere and Frey*, 1987]. Overall, the tholeiitic radial vent lavas show remarkably

Table 4. Representative XRF Whole Rock Compositional Analyses for Mauna Loa's Submarine Radial Vent and Other Submarine Lavas[a]

Vent Sample	North 1877 J2-14-11	South 1877 J2-18-12	Pa'ao J2-15-03	Kahole-a-kane J2-13-05B	Kua-o-wakea J2-13-07	Au'aulana M28-2[b]	Hinamolioli J2-18-08	Ka-wohi-kui-ka-moano M22-20[b]	C Flow J2-13-12
SiO_2	51.95	51.79	50.88	51.51	51.61	51.53	51.64	48.75	51.31
TiO_2	2.01	2.02	2.13	2.09	2.08	2.28	2.30	1.80	2.15
Al_2O_3	13.29	13.29	14.12	13.84	13.83	13.57	13.66	10.32	13.31
Fe_2O_3[c]	11.84	11.82	11.85	12.15	12.08	12.91	12.84	12.02	12.25
MnO	0.18	0.18	0.17	0.18	0.18	0.19	0.19	0.17	0.18
MgO	7.60	7.55	6.70	6.55	6.64	6.21	6.04	16.2	7.32
CaO	10.19	10.21	11.22	10.66	10.68	10.33	10.31	8.02	10.55
Na_2O	2.24	2.10	2.30	2.26	2.23	2.48	2.32	1.78	2.16
K_2O	0.36	0.36	0.37	0.38	0.38	0.47	0.46	0.301	0.34
P_2O_5	0.22	0.22	0.24	0.24	0.23	0.27	0.28	0.19	0.21
Total	99.87	99.52	99.97	99.87	99.94	100.24	100.03	99.57	99.78
Nb	8.2	8.1	8.9	9.2	9.1	10.1	10.2	7.6	8.9
Zr	125	124	136	136	135	146	149	114	128
Y	23.1	23.0	25.1	24.7	24.2	25.9	26.5	20.4	23.7
Sr	289	289	305	302	301	322	323	217	286
Rb	5.6	5.4	5.9	5.6	5.7	7	7.1	4.6	5.2
Ga	18	18	20	19	20	20	20	16	19
Zn	111	110	110	114	111	116	120	108	112
Ni	103	102	98	78	80	62	65	707	90
Cr	394	397	209	158	172	78	88	992	393
V	248	246	268	269	259	273	292	215	269
Ce	23	23	25	24	24	24	28	20	23
Ba	77	78	79	82	78	89	100	53	73

[a] Values in weight percent for oxides, ppm for trace elements.
[b] Dredge samples.
[c] Total iron.

similar trace element abundances except for Pb, which ranges from 0.7–2.9 ppm (Table 5). The high Pb values may be the result of low-temperature seafloor alteration [e.g., *Jochum and Verma*, 1996].

4.6. Sr, Nd, Pb, and He Isotope Data

[24] Pb, Sr, and Nd isotopic ratios were measured on 13 tholeiitic (Table 6) submarine radial vent samples the University of British Columbia, following procedures described by *Weis and Frey* [2002] and *Weis et al.* [2005]. The radial vent and other submarine lavas plot in a restricted portion of the isotope fields for Mauna Loa lavas (Figure 11). On a plot of $^{206}Pb/^{204}Pb$ versus $^{208}Pb/^{204}Pb$, the submarine lavas form a small, narrow field, whereas for $^{207}Pb/^{204}Pb$ there is one large group and two smaller groups (Figure 11). The high $^{207}Pb/^{204}Pb$ group consists of two flows (from the Akihimoana vent and an unknown source), whereas the two samples with low $^{207}Pb/^{204}Pb$ are the tholeiitic radial vent lava with the thickest sediment and Mn-Fe coating (Ka-wohi-kui-ka-moana), and the C flow lava. Although relatively small, the spread in $^{207}Pb/^{204}Pb$ ratios is comparable to what has been observed in the Mauna Loa part of Hawaii Scientific Drilling Project holes 1 [*Abouchami et al.*, 2000] and 2 [*Blichert-Toft et al.*, 2003; *Eisele et al.*, 2003], which span an age range of ~100 k.y. [*Sharp and Renne*, 2005].

[25] The Sr isotopes for the submarine Mauna Loa lavas display a relatively large range compared to analytical error and form two groups (Figure 12). The smaller group with lower Sr isotope ratios contains the C-flow sample (J2-13-13) and Ka-wohi-kui-ka-moana (M22-4), possibly the oldest radial vent lava. This low Sr isotope group plots with the older Mauna Loa lavas (Figure 13). The other group has higher Sr isotope ratios similar to the younger Mauna Loa flows (^{14}C-dated samples) [*Kurz et al.*, 1995]. Nd isotopes ratios for the submarine lavas show a more restricted range compared to Sr isotopes (Figure 12).

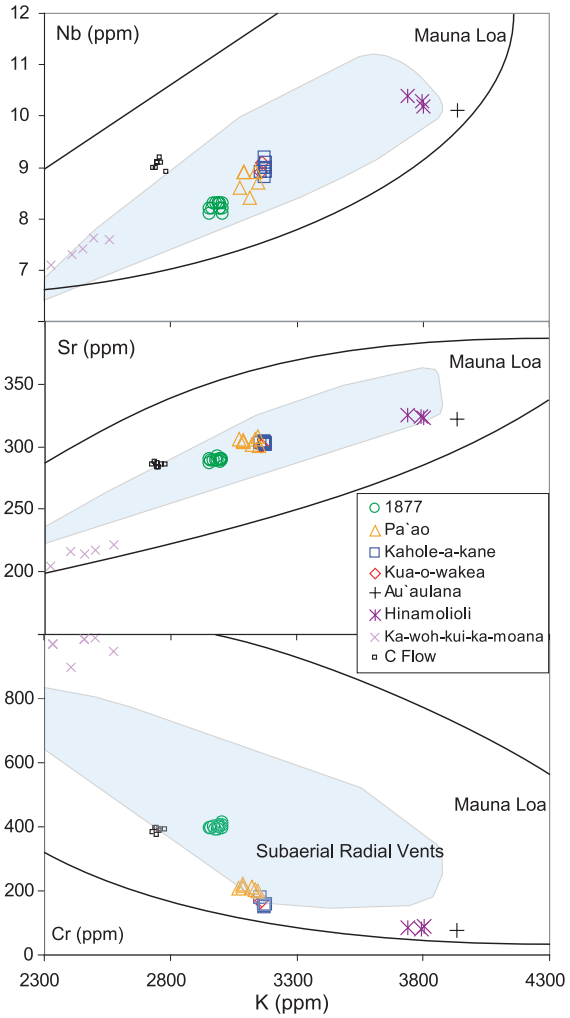

Figure 9. K variation diagrams for Cr, Sr, and Nb in Mauna Loa's submarine lavas. The field for the subaerial radial vents is shown in blue. The thick solid black line encloses the field for Mauna Loa lavas. Data for Mauna Loa fields from *Rhodes and Hart* [1995], *Rhodes* [1995], *Rhodes and Vollinger* [2004], and J. M. Rhodes (unpublished data). Analytical error is <1% for Cr, Sr, and Nb, and 1.5% for K [*Rhodes and Vollinger*, 2004].

[26] Helium isotopes in olivine melt inclusions and matrix glasses were measured by crushing in vacuo at Woods Hole Oceanographic Institution, using methods described by *Kurz et al.* [2004]. Only a handful of the samples have olivine phenocrysts or glassy material suitable for the helium measurements (see Table 7). The $^{3}He/^{4}He$ ratios in the radial vent samples vary from 8.4 to 17.6 times atmospheric (Ra), spanning nearly the entire range of previously reported values for Mauna Loa (8.0–20.0) [*Kurz and Kammer*, 1991; *Kurz et al.*, 1995].

5. Discussion

5.1. Radial Vent Ages

[27] Attempts were made to date three of the submarine radial vent samples (J2-13-06 from Kahole-a-kane, J2-14-04 from Akihimoana, J2-15-05 from Pa'ao) using unspiked K-Ar methods [*Guillou et al.*, 1997]. Sample J2-13-06 yielded an age of 7.5 ± 1.1 Ma, suggesting it contains mantle-derived excess argon. The two other samples yielded negative percentages of radiogenic argon (−0.4 to −0.2%) respectively slightly higher and within the range of similar results obtained for zero age reference material [e.g., *Scaillet and Guillou*, 2004]. The negative ages for the two radial vent samples provide support for the young ages inferred from other, less direct, methods. These approaches included geologic constraints, acoustic backscatter, sediment thickness, approximate ages from Mn-Fe coating thickness (using procedures from *Moore and Clague* [2004]) and He-Sr-Pb isotope data [*Kurz et al.*, 1995]. None of these methods provide accurate absolute ages, but taken together provide a consistent stratigraphic framework for the radial vent samples.

[28] The age limits for the submarine radial vent eruptions can be constrained by known geologic events. The most recent submarine eruption was witnessed in 1877 [*Whitney*, 1877]. An older age limit for one of the eruptions, Pa'ao, is based on its location within the Alika 2 landslide scar, which is thought to have formed between 115 to 127 ka [*McMurtry et al.*, 1999]. Pelagic sediment thicknesses have been used in previous studies [e.g., *Haymon et al.*, 1991] to determine relative ages on mid-ocean ridges far from land. However, Mauna Loa's submarine radial vents are located on the flanks of an island with high rates of sedimentation and mass wasting. Thus local variations in sediment thickness may compromise this method as a relative age indicator. With this caveat in mind, photographs taken with JASON2 cameras were used to estimate sediment thickness. Flows from each vent were assigned a number (1–5) that describes the amount of sediment draping the lava outcrops (Table 1). The flows with the thinnest amount of sediment (A.D. 1877) were given a value of one, whereas those with the most sediment (Hinamolioli) were ranked five. All other vents were given intermediate values.

Table 5. ICPMS Analyses of Mauna Loa's Submarine Radial Vent and Other Submarine Lavas[a]

Vent	1877		Pa'ao		Kahole-a-kane	Au'aulana	Hinamolioli	Ka-wohi-kui-ka-moana					C Flow	Other Flow	
Sample	J2-18-12	J2-14-12	M27-11[b]	J2-15-05	J2-13-06	M28-02R[b]	J2-18-07	M22-21[b]	M22-20[b]	M22-11R[b]	M22-17[b]	M22-04R[b]	J2-13-13	J2-14-10	J2-15-08
Li	4.9	4.7	5.0	5.1	5.2	5.8	6.0	4.6	4.6	4.6	4.6	4.4	4.9	5.7	5.5
Sc	30.6	29.8	31.7	33.0	31.3	33.0	32.4	25.5	25.4	25.0	24.9	23.5	31.0	25.7	31.3
V	249	239	263	272	258	294	296	225	223	222	221	208	261	288	274
Cr	386	374	-	221	152	-	80	-	-	-	-	-	357	92	302
Co	66	58	45	63	58	55	66	69	71	82	73	90	63	59	59
Ni	116	116	112	111	87	78	78	765	783	808	835	902	97	130	166
Cu	124	117	123	128	126	126	129	107	106	105	105	100	126	68	114
Zn	104	98	96	102	103	108	115	95	96	94	98	93	101	124	105
Ga	19.5	18.6	20.1	20.5	20.0	20.9	21.2	16.2	16.1	15.7	15.6	14.9	19.2	23.2	21.0
Rb	5.6	5.6	5.6	5.9	5.8	7.3	7.2	4.7	4.6	4.5	4.6	4.3	5.0	8.7	6.6
Sr	291	294	302	316	303	333	330	225	221	228	217	216	281	457	318
Y	23.0	22.3	24.5	25.8	24.5	26.9	27.1	20.8	20.5	20.8	20.2	19.5	22.9	29.9	27.0
Zr	120	117	127	134	131	146	146	111	110	111	109	104	119	180	143
Nb	8.3	8.4	8.5	9.3	9.0	10.5	10.6	7.7	7.6	7.7	7.5	7.3	9.0	13.7	10.2
Cd	0.078	0.076	-	0.077	0.077	-	0.081	-	-	-	-	-	0.074	0.084	0.075
Sn	1.7	1.6	1.5	1.6	1.6	1.7	1.9	1.3	1.3	1.3	1.2	1.2	1.5	2.1	1.7
Sb	0.025	0.025	0.022	0.029	0.030	0.027	0.045	0.022	0.022	0.022	0.020	0.019	0.042	0.044	0.046
Cs	0.063	0.059	0.061	0.068	0.068	0.079	0.086	0.049	0.048	0.050	0.048	0.045	0.060	0.094	0.086
Ba	84	80	76	82	86	101	108	60	59	60	59	56	75	122	97
La	8.8	8.3	9.0	9.5	9.5	11.0	11.7	7.6	7.5	7.5	7.5	7.0	9.0	13.7	10.7
Ce	22.8	21.5	23.1	24.5	24.7	28.0	29.8	19.5	19.6	19.5	19.4	18.3	23.4	35.2	27.4
Pr	3.51	3.29	3.57	3.76	3.74	4.14	4.44	2.95	3.00	2.94	2.97	2.79	3.50	5.25	4.14
Nd	17.0	15.9	17.0	18.0	17.9	19.6	20.8	14.4	14.3	14.4	14.1	13.5	16.6	24.6	19.6
Sm	4.94	4.61	4.87	5.19	5.12	5.58	5.79	4.17	4.21	4.24	4.17	3.91	4.83	6.76	5.56
Eu	1.71	1.62	1.75	1.79	1.75	1.93	1.98	1.43	1.42	1.42	1.43	1.34	1.67	2.29	1.87
Gd	5.42	5.16	5.65	5.74	5.47	6.20	6.33	4.73	4.71	4.89	4.68	4.51	5.13	7.02	6.00
Tb	0.88	0.83	-	0.93	0.89	-	1.02	-	-	-	-	-	0.84	1.12	0.97
Dy	4.93	4.72	5.10	5.29	5.06	5.56	5.77	4.48	4.35	4.43	4.27	4.22	4.85	6.32	5.55
Ho	0.96	0.93	1.01	1.04	0.99	1.08	1.12	0.88	0.87	0.86	0.84	0.80	0.95	1.23	1.09
Er	2.38	2.31	2.58	2.57	2.48	2.71	2.80	2.19	2.17	2.12	2.13	1.99	2.38	3.04	2.72
Yb	2.01	1.95	2.12	2.18	2.10	2.27	2.39	1.85	1.83	1.83	1.83	1.72	2.00	2.62	2.33
Lu	0.28	0.28	0.31	0.31	0.29	0.33	0.34	0.26	0.25	0.26	0.25	0.24	0.28	0.37	0.33
Hf	3.19	3.11	3.37	3.39	3.34	3.73	3.80	3.01	2.98	2.90	2.92	2.76	3.13	4.62	3.58
Pb	0.79	0.79	0.83	1.27	1.41	1.07	2.72	0.68	0.69	0.78	0.68	0.74	3.07	1.47	2.74
Th	0.56	0.54	0.56	0.61	0.62	0.68	0.72	0.50	0.50	0.50	0.49	0.47	0.65	0.88	0.70
U	0.20	0.19	0.18	0.21	0.21	0.22	0.25	0.16	0.16	0.16	0.16	0.15	0.22	0.30	0.23

[a] All values in ppm; analyst: M. Norman.
[b] Dredge samples [*Davis et al.*, 2003].

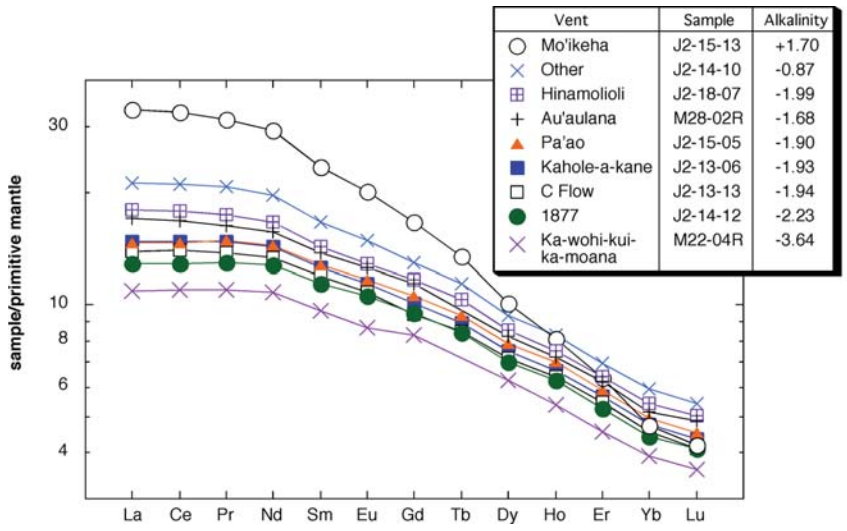

Figure 10. Primitive mantle normalized REE plot for selected Mauna Loa submarine radial vent lavas. The mild fanning of the LREE patterns and crossing HREE patterns cannot be explained by low pressure fractionation. These features probably represent small variations in partial melting in the garnet peridotite stability field. The sample with the highest LREE concentrations also has the highest alkalinity [total alkalis-((SiO_2 × 0.37) − 14.43)]. Primitive mantle normalizing values are from *McDonough and Sun* [1995]. Accuracy and precision were <1 to 2% for all elements based on repeat analyses of several samples.

[29] A second method of relative dating utilized acoustic backscatter data. In backscatter images, lava flows normally appear highly reflective (dark; Figure 3), whereas sedimented areas are less reflective and have lower backscatter [*Applegate*, 1990]. This approach can be complicated by topography and "look" direction of sonar insonification, which can alias backscatter strength [*Applegate*, 1990]. The volcanic surface roughness and the local slope are the primary factors in determining backscatter strength (i.e., high roughness and steep slopes produce high backscatter in the acoustic images) [e.g., *Applegate*, 1990; *Hagen et al.*, 1990]. Despite these potential problems, backscatter data can help to infer the relative ages of the radial vent deposits. The submarine radial vents were divided into three categories based on reflectivity (Figure 3). The order of high to low reflectivity matches the order assigned based on sediment thickness using JASON2 photographs (high, <3; medium, 3–4; and low, 5) except for the C flow, which is transitional (Table 1).

[30] Mn-Fe coatings have been used to estimate ages for Hawaiian submarine basalts based on an average rate of growth of ~2.5 mm/m.y. around the Hawaiian Islands [*Craig et al.*, 1982]. These coatings begin to form upon exposure to seawater [*Moore and Clague*, 2004]. Microscopic thicknesses of Mn-Fe coatings as thin as 0.015 mm have proven useful in dating young Hawaiian basalts (6 to 380 ka) [*Moore and Clague*, 2004]. Thin patches of Mn-Fe coatings were found on some submarine radial vent and flow field glasses (Table 1). The thickest coatings are on a Ka-wohi-kui-ka-moana vent lava (0.118 ± 0.001 mm) and a Hinamolioli vent sample (max. 0.078 ± 0.001 mm), yielding age estimates of ~47 ka and ~31 ka. The other submarine lavas have thinner coatings (max. 0.029 to 0.049 ± 0.001 mm), corresponding to ages of ~12 to 20 ka (Table 1). The age sequence based on Mn-Fe coatings is consistent with the sequences inferred from backscatter and sediment thickness estimates except for Au'aulana, which has less reflectivity than anticipated on the basis of its Mn-Fe coating thickness (Table 1).

[31] An additional age constraint is obtained by comparing the isotope geochemistry of the radial vent samples with ^{14}C-dated subaerial Mauna Loa lavas, which show a large and systematic temporal isotopic variation [*Kurz and Kammer*, 1991; *Kurz et al.*, 1995]. Flows older than 28 ka have higher $^{3}He/^{4}He$ and $^{206}Pb/^{204}Pb$ and lower $^{87}Sr/^{86}Sr$ than younger flows (Figure 13). The isotopic ratios of these dated flows overlap with those of the radial

Table 6. Pb, Sr, and Nd Isotope Analyses of Mauna Loa's Submarine Tholeiitic Radial Vent and Other Submarine Lavas

Vent	Sample	$^{206}Pb/^{204}Pb$	2 sigma	$^{207}Pb/^{204}Pb$	2 sigma	$^{208}Pb/^{204}Pb$	2 sigma	$^{87}Sr/^{86}Sr$	2 sigma	$^{143}Nd/^{144}Nd$	2 sigma
1877	J2-18-12	18.1502	0.0016	15.4621	0.0013	37.8999	0.0036	0.703851	0.000007	0.512907	0.000006
	J2-14-12	18.1502	0.0023	15.4607	0.0018	37.8955	0.0045	0.703839	0.000007	0.512896	0.000008
Paʻao	J2-15-5	18.1381	0.0016	15.4626	0.0015	37.8841	0.0036	0.703761	0.000008	0.512926	0.000006
	M27-2[a]	18.1377	0.0013	15.4615	0.0011	37.8839	0.0028	0.703773	0.000009	0.512936	0.000004
	M27-11[a]	18.1362	0.0014	15.4606	0.0013	37.8744	0.0034	0.703773	0.000005	0.512941	0.000008
Kahole-a-kane	J2-13-06	18.1407	0.0019	15.4587	0.0017	37.8871	0.0040	0.703800	0.000007	0.512915	0.000006
Kua-o-wakea	J2-13-08	18.1396	0.0018	15.4581	0.0017	37.8862	0.0041	0.703821	0.000008	0.512913	0.000006
Auʻaulana	M28-2[a]	18.0956	0.0019	15.4632	0.0016	37.8808	0.0041	0.703890	0.000008	0.512887	0.000005
Hinamolioli	J2-18-7	18.0935	0.0017	15.4613	0.0014	37.8761	0.0039	0.703885	0.000006	0.512891	0.000007
Ka-wohi-kui-ka-moano	M22-4[a]	18.1769	0.0030	15.4497	0.0028	37.9090	0.0063	0.703670	0.000006	0.512959	0.000007
C Flow	J2-13-13	18.1769	0.0025	15.4482	0.0022	37.8909	0.0053	0.703684	0.000007	0.521964	0.000007
Other Flows	J2-14-10	18.1172	0.0011	15.4577	0.0009	37.8687	0.0024	0.703799	0.000006	0.512919	0.000007
	J2-15-8	18.1884	0.0013	15.4718	0.0013	37.9325	0.0033	0.703799	0.000008	0.512935	0.000006

[a] Dredge samples; analyst: D Weis.

vent lavas, and thus are potentially useful in defining broad age groups based on two assumptions: 1. Mauna Loa's temporal evolution is represented by existing data; and 2. the volcano's isotopic evolution has been monotonic, especially for the period between 12 and 28 ka where these is a data gap (Figure 13). The sample from the 1877 flow has relatively low $^{3}He/^{4}He$ (8.4 Ra) and moderate $^{87}Sr/^{86}Sr$, overlapping with the historical group, whereas samples from the C-flow (J2-13-13) and Ka-wohi-kui-ka-moano vent (M22) have significantly higher $^{3}He/^{4}He$ ratios (16.8–17.6 Ra) and lower $^{87}Sr/^{86}Sr$, overlapping with the >28 ka group. Samples from the Paʻao vent (M27-02) and the two alkali basalt flows (J2-15-13 and J2-14-04) have intermediate $^{3}He/^{4}He$ values (11.7–14.7 Ra; Table 7) overlapping with the 7–12 ka group. These age groups (Table 7) are consistent with all three isotope systems but are most obvious in the Sr-He diagram, because there is almost complete overlap between historical and 7–12 ka flows in Sr

Figure 11. Pb isotope ratio plots for Mauna Loa's submarine lavas. These lavas have similar Pb isotope signatures to other Mauna Loa lavas (fields from D. Weis, unpublished data). The submarine data form a single elongate field for $^{208}Pb/^{204}Pb$. In contrast, the $^{207}Pb/^{204}Pb$ data reveal three separate groups. The higher $^{207}Pb/^{204}Pb$ samples are a tholeiitic lava not from radial vent and an Akihimoana alkalic lava. The two low $^{207}Pb/^{204}Pb$ ratios are from the oldest (~47 ka) submarine radial vent (based on Mn-coating thickness) and the C flow. Analytical errors are smaller than the symbols for all Pb analyses. See Table 6 for data.

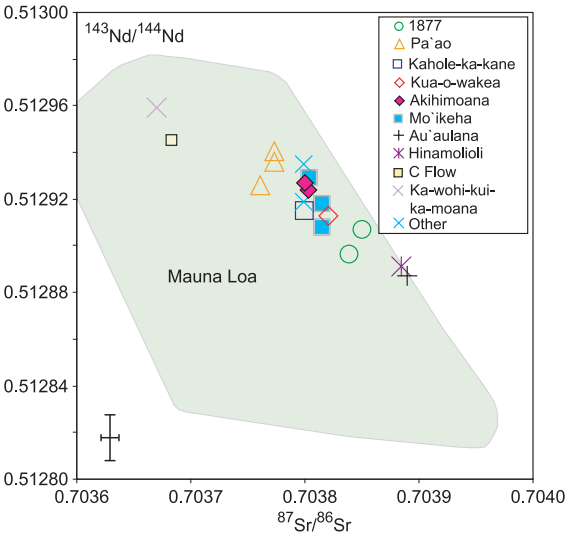

Figure 12. Nd and Sr isotope plot for Mauna Loa submarine radial vents and other lavas. Nd isotopes show a restricted range forming one elongate group. The Sr isotope data form two groups. The smaller group with lower Sr isotope ratios contains the C-flow sample (13-13) and the oldest radial vent lava (M22-4). This group plots with the older Mauna Loa lavas [*Kurz et al.*, 1995; D. Weis, unpublished data], whereas most of the radial vent lavas plot along a Nd-Sr isotope trend similar to the ^{14}C dated samples of *Kurz et al.* [1995]. See Table 6 for data.

and Pb isotopes (Figure 13). The relative ages based on the He-Sr-Pb isotopes are consistent with those from the other methods, although they are somewhat younger than those inferred from the Mn-Fe crusts (Table 1). These results indicate that the submarine radial vents may span an age range from 128 years (1877 A.D.) to ~47 ka, greatly extending the known history of Mauna Loa radial vent eruptions, and they provide a framework for evaluating geologic processes in the Kealakekua Bay area.

5.2. Compositional Heterogeneity and Temporal Trends?

[32] The submarine radial vent lavas span wide ranges in mineralogy, major and trace elements, and Pb, Sr, Nd and He isotopes (Table 2; Figures 7 and 11–13). These results and modeling using the MELTS program (Figure 7) indicate many distinct parental magmas were involved in producing these lavas. This may reflect the rapid changes that have also been observed for historical Mauna Loa and Kilauea lavas [*Rhodes and Hart*, 1995; *Pietruszka and Garcia*, 1999]. However, two pairs of vents have similar geochemistry and relative ages. The two adjacent vents (Kahole-a-kane and Kua-o-wakea) are petrographically and geochemically identical (Tables 2–4 and 6), and have nearly identical relative ages based on sediment thickness and reflectivity (Table 1). They are probably related to the same eruptive sequence. Two older vents in the northern part of the study area (Figure 2), Auaulana and Hinamolioli, may also be related to the same parental magmas. However, the lavas from the two alkalic vents are geochemically distinct [*Wanless et al.*, 2006]. Thus, although some vents may be related to the same parental magma, there is a marked compositional heterogeneity among the submarine radial vent lavas.

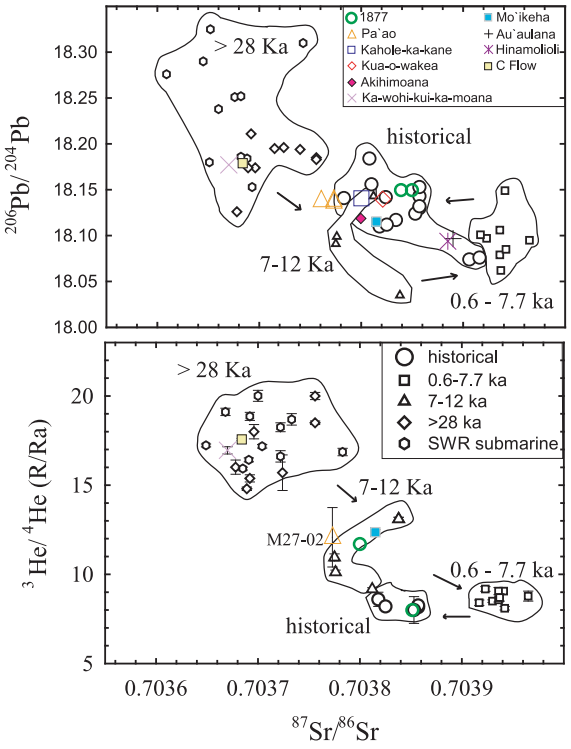

Figure 13. Sr, Pb, and He isotopic data for the submarine radial vents compared to Mauna Loa ^{14}C-dated subaerial lava flows and submarine southwest rift zone lavas. The submarine southwest rift samples are thought to be >31 ka [*Garcia et al.*, 1995]. The distinct Sr-Pb-He isotopic compositions for the ^{14}C-dated subaerial Mauna Loa flows provide age constraints for the radial vent glasses, based on the assumption that the subaerial dated flows adequately represent the isotopic evolution of Mauna Loa. Radial vents (solid circles) have sample numbers next to the symbol. The data for the subaerial and submarine southwest rift zone lavas are from *Kurz and Kammer* [1991] and *Kurz et al.* [1995]. See Tables 6 and 7 for new data.

Table 7. Helium Isotope Data From Submarine Radial Vent Samples[a]

Sample	Phase	Weight, g	^{4}He, nano-cc/g	^{3}He/^{4}He, R/Ra	±	Vent	Model Age, ka
J2-18-12	glass	0.10456	19	8	0.1	1877	historical
J2-18-05	glass	0.25	28.5	8.4	0.1	1877	historical
M27-02[b]	glass	0.28936	0.106	12.1	1.7	Pa'ao	7–12
J2-14-04	olivine	0.2425	8.55	11.7	0.1	Akihimoana	7–12
J2-15-13	olivine	0.13337	5.4	12.4	0.1	Mo'ikeha	7–12
M22-4	olivine	0.29773	1.86	16.6	0.2	Kawohi-kui-ka-moana	>28
M22-11	olivine	0.28525	2.79	16.9	0.2	Kawohi-kui-ka-moana	>28
M22-02	olivine	0.24395	3.54	17	0.2	Kawohi-kui-ka-moana	>28
M22-02[b]	glass	0.21818	1.52	14.7	0.3	Kawohi-kui-ka-moana	>28
J2-13-13	glass	0.2729	474.2	17.6	0.1	C flow	>28

[a] All measurements by crushing in vacuo. Model ages based on combined He-Sr-Pb isotope data for ^{14}C dated subaerial lavas (see text and Figure 13).
[b] Low concentration glasses; ^{3}He/^{4}He values are lower limits.

[33] Is there systematic compositional variation among Mauna Loa's submarine radial vent lavas span, which span wide age (118 years to ~47 ka) and compositional ranges (alkalic to tholeiitic; Table 1; Figures 7, 11, and 12)? The lavas from the oldest vent (Ka-wohi-kui-ka-moana) and the C flow have higher, He, Nd and ^{206}Pb/^{204}Pb, and lower Sr isotope ratios than other submarine samples (Figure 13), geochemical features typical of older Mauna Loa flows [*Kurz et al.*, 1995]. The 1877 lavas are geochemically distinct with the lowest ^{3}He/^{4}He ratios (Table 7), although they have intermediate values for other isotopes and incompatible element ratios. Among the other tholeiitic lavas, two older vents with similar relative ages, Auaulana and Hinamolioli (Table 1), have the lowest ^{143}Nd/^{144}Nd and ^{206}Pb/^{204}Pb values, and the highest ^{87}Sr/^{86}Sr and K/Y ratios (Figures 11, 12, and 14). The other intermediate age lavas show no apparent temporal geochemical variation but are distinct from other radial vent lavas (Figures 7, 11, and 12). Of particular importance, the compositions of these lavas show no systematic increase in alkalinity (Figure 10) with age as would be expected if Mauna Loa was dying [e.g., *Rhodes and Vollinger*, 2004]. Overall, He isotopes provide the best evidence for temporal geochemical variation among the radial vent lavas (Table 7, Figure 13), as observed for subaerial lavas [*Kurz et al.*, 1995].

[34] Mauna Loa historical subaerial lavas display a systematic temporal variation, which was rapid between 1840 and 1880 (Figure 15). The geochemistry of lavas from the submarine 1877 eruption plots on this trend with similar compositions to the northeast rift zone eruption of 1880 and distinct from earlier 19th century and 20th century lavas (Figure 15). The strong similarity of the lavas from the 1877 and 1880 eruptions on opposite sides of the volcano, and the rapid variation in Mauna Loa lavas before and after these eruptions, suggests that both eruptions were probably derived from the same, rapidly changing reservoir. Thus the 1877 and possibly other tholeiitic radial vents may have been fed from the summit reservoir just prior to their eruptions rather than from independent conduits from the mantle.

5.3. Influence of Major Element Composition on Crystallization Sequence

[35] Crystallization sequences in lavas provide insights into their magmatic history. Olivine is expected to be the liquidus mineral in Hawaiian tholeiitic magmas at crustal depths [e.g., *Wright*, 1971]. The next phase to crystallize is dependent upon the magma's bulk composition. For Mauna Loa compositions, one atmosphere experiments showed that plagioclase crystallizes second (at ~1160°C), followed by cpx (~1150°C) and pigeonite (~1140°C) [*Montierth et al.*, 1995]. The petrography of most of the submarine radial vent lavas record this sequence, except for pigeonite, which is absent (Table 2). The 1877 lavas, however, follow a different crystallization sequence with opx crystallizing as the second phase.

[36] The early appearance of opx in the crystallization sequence for 1877 lavas is probably related to their somewhat different bulk composition (Table 4). To evaluate the crystallization trends for historical Mauna Loa magmas, the MELTS program [*Ghiorso and Sack*, 1995] was employed using lavas from the 1843 and 1880 eruptions as possible parents. These lavas span the post-1832 compositional range for Mauna Loa [*Rhodes and*

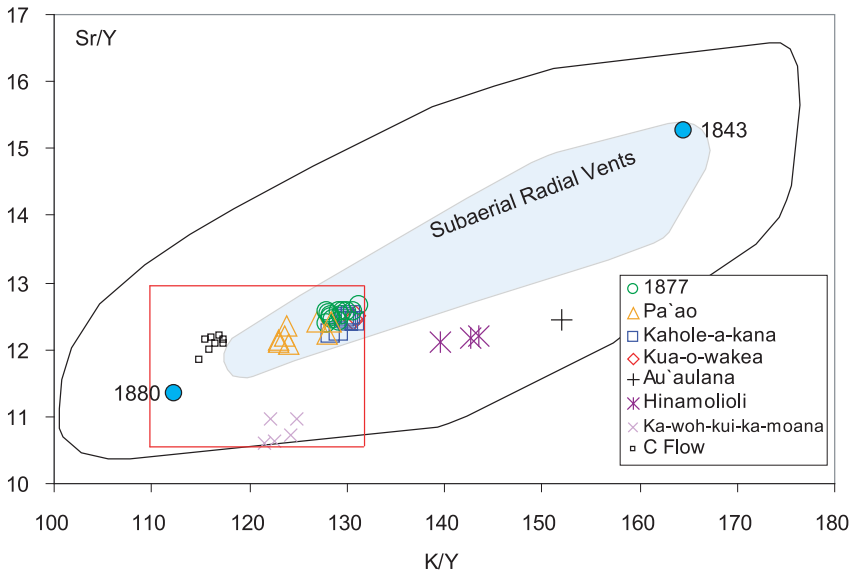

Figure 14. Sr/Y versus K/Y for Mauna Loa submarine lavas. The field for the subaerial radial vents is shown in blue. The thick solid black line encloses the field for Mauna Loa lavas. The two post-1832 Mauna Loa end-member compositions are shown as blue circles (1880 and 1843) [*Rhodes and Hart*, 1995]. The 1880 sample, which is thought to represent periods of high eruption rates, has low Sr/Y and K/Y ratios. The red box represents the compositional range that is thought to be dominated by lavas formed during higher eruption rates [*Rhodes and Hart*, 1995]. Most submarine lavas fall within this box, including the picritic lavas from Ka-wohi-kui-ka-moana, which have Sr/Y compositions lower than any other submarine radial vent lava.

Hart, 1995]. Attempts at modeling the magmatic history of the 1877 lava using an 1843 parental composition were unsuccessful. No variations in the MELTS modeling parameters (oxygen fugacity, pressure, and water content) yielded opx as the second phase to crystallize. Plagioclase always formed before opx, as was found in the experimental study by *Montierth et al.* [1995]. In contrast, the 1880 parent, with its slightly lower CaO/Al_2O_3 (Figure 7), crystallized opx second, followed by plagioclase and cpx, as observed in the 1877 lavas. Thus a small difference in bulk composition is apparently sufficient to shift the opx cotectic to allow it to crystallize second in the 1877 lavas. This result is of importance in studying lavas from other volcanoes to avoid unnecessarily invoking a process or variation in an extrinsic parameter [e.g., *Clague and Dixon*, 2000] to explain variations in crystallization sequences.

5.4. Degassing History of Radial Vent Magmas

[37] The sulfur content of basaltic glass has been shown to be a useful indicator of depth of a submarine eruption [e.g., *Moore and Fabbi*, 1971]. Degassing in Hawaiian magmas typically begins at crustal depths of ~300 m or water depths of ~1000 m for Hawaiian basalts [e.g., *Mathez*, 1976]. Most of the glasses from the Mauna Loa submarine radial vent lavas are degassed (the

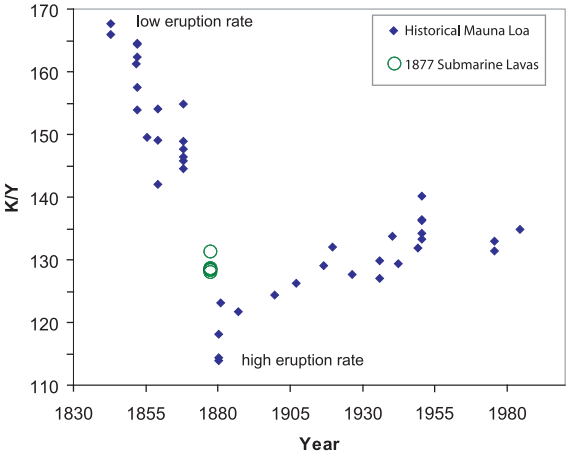

Figure 15. Temporal variation in K/Y for Mauna Loa historical lavas (post-1832). The 1877 submarine radial vent lavas fall on this trend, which was changing rapidly during the 19th century. This suggests that magma for the 1877 eruption was tapped from the summit reservoir just before it erupted. Data for historical lavas from *Rhodes and Hart* [1995].

exceptions are 1877 and Akihimoana lavas; Figure 8) despite having been erupted at depths of 900 to 2,200 mbsl, which should have inhibited degassing [*Moore and Fabbi*, 1971]. Glass inclusions in the rare euhedral olivine and plagioclase phenocrysts in several of these degassed lavas were analyzed and found to contain undegassed levels of S (>900 ppm). Thus the magmas for these lavas lost their volatiles late in their crystallization history. The low S content of radial pillow rim glasses is not related to subsidence of the lavas after quenching since they probably subsided <130 m, given the slow rate of island subsidence (~2.5 mm/yr) [*Moore et al.*, 1990] and their relatively young ages (<50,000 years; Table 1). Many of the subaerial radial vents lack near-vent structures, which *Lockwood and Lipman* [1987] interpreted as indicative of eruption of degassed magma. These subaerial lavas are thought to have been originally degassed at the summit, perhaps during a period of extensive lava lake activity, and then drained out the side of the volcano [*Lockwood and Lipman*, 1987]. The degassed submarine radial vent magmas may have had a similar degassing history indicating that a shallow fracture propagated at least 40 km from the summit reservoir to fed the submarine eruptions.

5.5. Radial Vent Cone Shape

[38] Near the Hawaiian Islands, multibeam data [*Clague et al.*, 2000] and Gloria side scan images [*Bridges*, 1997] were utilized to describe 524 submarine cones. Most (328 or 63%) were categorized as flat-topped (Figure 16) due to their low aspect ratios (height/basal diameter <0.14), nearly horizontal tops (only 10–20 m of offset from one edge to the other), and steep flanks (>25°) [*Rappaport et al.*, 1997]. The second most common cones around the islands are "pointed cones" (aspect ratios of 0.11 to 0.25) [*Clague et al.*, 2000]. These cones have low flatness ratios (minimum summit diameter to minimum basal diameter; ~0.03) and moderate slopes (5–15°), and lack summit craters [*Rappaport et al.*, 1997]. They are thought to be associated with post-shield alkalic volcanism [*Clague et al.*, 2000]. Other types of submarine constructs near the Hawaiian Islands include heaps, truncated cones, shields, and star-shaped seamounts [*Bridges*, 1997].

[39] Among Mauna Loa's ten shield-stage submarine radial vents, only one (Ka-wohi-kui-ka-moana) has the low aspect ratio (0.1; Table 1) and steep flanks of a flat-topped cone. The other

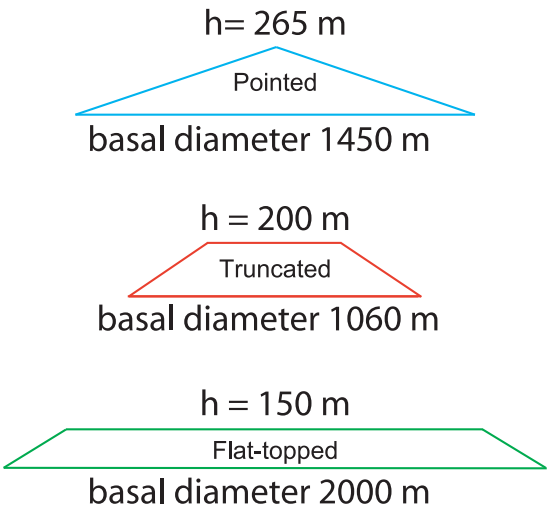

Cone Shapes	Flat-topped	Truncated	Pointed
aspect ratio	<0.14	0.14-0.28	0.11-0.25
flatness	0.01-0.57	0.25-0.57	<0.03
slope	>25	>20	5-15
summit depression	sometimes	sometimes	no
degassed	yes	no	no

Figure 16. Schematic diagram depicting the shape differences between submarine Hawaiian flat-topped, pointed, and truncated cones. The flat-topped and pointed cones are drawn using the average cone dimensions from *Clague et al.* [2000]. The ranges for aspect ratio, flatness, slope, presence of summit depression, and whether glasses are degassed from these cones are from *Clague et al.* [2000]. The truncated cone dimensions and ranges are an average of the Mauna Loa submarine radial vent cones. The cone height is shown as "h."

radial vents have higher aspect (0.14 to 0.28) and flatness ratios (0.25 to 0.57 excluding Hinamolioli, whose base is covered by the 1877 flows; Table 1). The summits of seven submarine radial vent cones are truncated and four of these contain well-developed summit craters (Figure 2). Therefore these seven are neither flat-topped nor pointed cones; they are best described as truncated cones (Figure 16). The irregular shapes of two cones (1877 and Akihimoana) do not fit in any previously described cone shape category. Both cones produced undegassed lavas and flows >3 km long. Thus these eruptions were of a different style.

[40] Submarine cone shape is thought to be controlled by many parameters, including viscosity of the erupting magma, effusion rate, initial magmatic volatile content, separation of the gas phase, erup-

tion duration, lava composition and water depths [*Clague et al.*, 2000]. The formation of a flat-topped cone is considered to require prolonged low to moderate effusion of magma with low viscosities and volatile content on gentle slopes [*Clague et al.*, 2000]. However, Mauna Loa truncated cones formed under many of these same conditions. For example, they were found at similar water depths and on moderate- to low-angle slopes (Figures 2 and 4). Also, glass S analyses reveal that both the radial vent flat-topped and truncated cones erupted degassed lavas (Figure 8) and the viscosity of the lavas from these cones were probably similar (20 to 170 Pa s), given their similar major element compositions and volatiles, and their low crystallinity. Therefore the development of truncated versus flat-topped cones cannot be related to these parameters. Effusion rate and/or eruption duration may be the key factors in determining cone shape but these parameters are unknown for the Mauna Loa submarine lavas.

[41] Volatile content is thought to play an important role in the formation of pointed rather than flat-topped or truncated cones [*Clague et al.*, 2000]. Pointed cones around the Hawaiian Islands have circular bases and are assumed to be composed of alkalic lavas because volatile exsolution during eruption is envisioned to produce fragmental ejecta creating a pointed structure [*Clague et al.*, 2000]. The two more volatile-rich eruptions, one tholeiitic (1877) and the other alkalic (Akihimoana), formed irregular cones with extensive lava flows (Figure 6). The relatively low vesicularity (0.2 to 8 vol.%) and high S content (>0.06 wt%) of these tholeiitic and alkaline lavas suggests most of the volatiles remained dissolved in the lava prior to quenching. Thus eruption of undegassed magma may hinder formation of symmetrical cone. In contrast, eruption of degassed magma seems to have favored formation of truncated cones. All seven of the radial vents with degassed glasses formed truncated cones.

[42] It has been argued that the amount of volatiles dissolved in a submarine lava affects the travel distance of a lava flow [*Gregg and Fornari*, 1998; *Clague et al.*, 2000]. Seven of Mauna Loa's submarine radial vents have associated lava flows, although only flows from the 1877 and Akihimoana vents traveled farther than three km (Figure 6). The high S content of the glasses (Figure 8, Table 3) from these long flows supports the hypothesis that dissolved volatiles enhance submarine lava flow lengths [e.g., *Gregg and Fornari*, 1998].

5.6. Implications of Volume Estimates

[43] Mauna Loa's 1877 eruption was previously estimated to be small ($\sim 8 \times 10^6$ m^3) and short (<1 day), based on eyewitness accounts [*Lockwood and Lipman*, 1987; *Barnard*, 1995]. Our new bathymetric, acoustic backscatter, ROV video and sampling data show that the 1877 eruption was much larger (434×10^6 m^3; Table 1), making it Mauna Loa's second largest post-1832 eruption. The large 1877 flow field (Figure 6) is unlikely to have formed in a single day given Mauna Loa's typical eruption rate (e.g., 110 m^3/sec for the 1984 eruption) [*Lockwood et al.*, 1987]. Even with the highest inferred Mauna Loa eruption rates ($\sim$1,000 m^3/sec) [*Rowland and Walker*, 1990], five days are needed to produce the voluminous 1877 flow field.

[44] The new volume for the 1877 eruption increases the estimate for Mauna Loa's post-1832 eruption rate by $\sim$10%, from 29×10^6 m^3/yr [*Lockwood and Lipman*, 1987] to 32×10^6 m^3/yr. This rate is comparable to the average rate for Kīlauea volcano during the last two hundred years ($\sim 34 \times 10^6$ m^3/yr), although Kīlauea's rate has been highly variable (5 to 100 $\times 10^6$ m^3/yr) [*Pietruszka and Garcia*, 1999]. The new volume estimates, together with the ongoing inflation and seismicity at Mauna Loa indicate that the prediction that the volcano is near the end of its shield stage [*Moore et al.*, 1990; *Lipman*, 1995] may be premature. These results also indicate that the recent radial vent eruptions (1852, 1859, and 1877) have played a significant role in the growth of the volcano, accounting for 22% of the volume of lava produced since 1832.

[45] Another outcome of the volume estimates is that submarine radial vent eruptions tend to be large, although highly variable, in volume (10 to 430×10^6 m^3; Table 1). For example, the average lava volume of a submarine radial vent is substantially larger than the average post-1832 subaerial eruption on Mauna Loa (226×10^6 m^3 versus 129×10^6 m^3) [*Barnard*, 1995]. Furthermore, few (5/33; 15%) post-1832, non-radial vent eruptions produced volumes greater than 200×10^6 m^3 [*Lockwood and Lipman*, 1987], compared to most (5/9; 56%) submarine radial vent eruptions. Thus radial vent eruptions are important contributors to the submarine growth of Mauna Loa.

5.7. Submarine Growth of Mauna Loa

[46] The discovery of numerous radial vents on the submarine flanks of Mauna Loa has implica-

tions for models explaining the submarine construction of Hawaiian shield and other oceanic island volcanoes. A debate exists on the relative proportions of lava flows and fragmental debris that comprise the submarine flanks of these volcanoes [e.g., *Fornari et al.*, 1979; *Fornari*, 1986; *Moore and Chadwick*, 1995; *Garcia and Davis*, 2001]. On the basis of bathymetric data collected around the island of Hawai`i, as well as observations from two recent eruptions from Kīlauea volcano, *Moore and Chadwick* [1995] suggested that the flanks of Hawaiian volcanoes are composed primarily of fragmental debris. During submersible dives on the flanks of Mauna Loa (at depths of 1–2 km), *Garcia and Davis* [2001] observed predominantly pillow lavas in rock sections. The top of these sections and other gently to moderately-dipping surfaces are commonly draped with many decimeters to meters of mud masking underlying pillow lavas from being detected by acoustic backscatter and other remote sensing techniques.

[47] Although ~2/3 of the Kealakekua Bay area is draped with sediment, all of the outcrops are pillow lava or sheet flows. No outcrops of hyaloclastite or any other form of fragmental volcanic debris were observed in any of the many sections we examined. However, along the ~28 km of the coastline adjoining the study site, only one coherent lava flow was observed in backscatter images to have crossed the shoreline in the southernmost part of the map area (Figure 6). It extends offshore for ~3.5 km. There are three lava fields with no obvious submarine source vent or landward connection, which account for ~25% of the lava flows in the study area (Figure 6). However, flows from submarine radial vents account for most of the lava in this area (>70%). Glasses from the eight of these mapped units are degassed (Figure 8). Thus submarine radial vents offer an additional method for emplacing degassed magma on to the submarine flanks of Mauna Loa. Regardless of whether these flows erupted subaerial or from submarine radial vents, our new acoustic imagery and video surveys combined with previous submersible observations [e.g., *Fornari et al.*, 1979, 1980; *Moore and Clague*, 1987; *Garcia and Davis*, 2001] document that pillow lavas represent an important rock type on the flanks of Mauna Loa. Similar studies are needed of other oceanic volcanoes to document whether Mauna Loa is representative of oceanic volcanoes.

5.8. Radial Vent Activity Versus Eruption Rate?

[48] Mauna Loa's eruptive activity over the last 4,000 years has been cyclical, alternating from periods dominated by rift zone to summit eruptions [*Lockwood and Lipman*, 1987]. When the summit was active, it was characterized by nearly continuous lava lakes and voluminous overflows, and was a time of rapid shield-building [*Lockwood*, 1995]. Subaerial radial vent eruptions were more common during periods of sustained summit eruptions, although no evaluation was made between overall eruption rate and radial vent activity [*Lockwood and Lipman*, 1987]. It may not be coincidental, however, that the historical radial vent eruptions in 1852, 1859, 1877 occurred during a period of high eruption rate (1843–1880). Unfortunately, this model cannot be tested in detail because all but one of the submarine radial vent eruptions predate the relatively recent period for which eruption rates have been inferred from field evidence.

[49] Alternatively, it may be possible to infer eruption rates from geochemical variations. Fluctuations in Mauna Loa's eruption rate over the last 160 years correlate with incompatible element abundances and ratios in its lavas [*Rhodes and Hart*, 1995]. For example, during periods of low magma supply and eruptive activity, higher K/Y and Sr/Y values are observed than during period of high magma supply (Figure 15). The inverse correlation between eruption rate and magma enrichment could reflect periods of increased melting and/or melting of refractory source components resulting in higher eruption rates and lower incompatible element ratios [*Rhodes and Hart*, 1995]. A similar inverse correlation was noted for Kīlauea's historical lavas [*Pietruszka and Garcia*, 1999]. Incompatible trace element ratios for most submarine radial vent lavas are relatively low, with the more voluminous submarine radial vent eruptions (>300 $\times$ 10^6 m^3) having the lowest K/Y ratios (<132; Figure 14). These results indicate a more depleted source and suggest the submarine radial vent eruptions occurred during periods of higher magma supply and eruptive activity.

6. Summary

[50] The discovery of nine new vents on Mauna Loa's submarine western flanks has increased the volcano's known radial vent population from 45 to 54 (20%). Our detailed geologic map indicates that

Mauna Loa's western submarine flank was the site of multiple effusive eruptions, producing $\sim 2 \times 10^9$ m^3 of lava. These results support the idea that pillow lavas are an important component of oceanic island volcanoes, even after they emerge above sea level. The map also shows that the 1877 eruption was much larger than previously thought, increasing the post-1832 eruptive volume of Mauna Loa by 10%. Furthermore, although alkalic lavas were found at two radial vents, there is no systematic increase in alkalinity among these or other Mauna Loa lavas as expected for a dying volcano. Thus the prediction that Mauna Loa may be nearing the end of its shield stage is premature.

[51] The new detailed bathymetric and geochemical data allow characterization of the physical characteristics and geology of Mauna Loa's submarine radial vent cones. The west flank of this shield contains three types of submarine cones: flat-topped, truncated, and irregular. Although flat-topped cones are common around the Hawaiian Islands, only one was found on the west flank of Mauna Loa. Instead, truncated cones are the dominant cone shape and all produced degassed lavas. The presence of higher volatile contents in glasses from two irregular shaped radial vents correlates with longer lava flow length. Thus higher volatile content in shield lavas may result in longer submarine lava flows, as predicted on theoretical grounds.

[52] A variety of techniques were used to establish a temporal sequence for the radial vent lavas. The ages for these vents range from 1877 to possibly 47 ka. Thus the radial vent lavas span wide age as well as compositional ranges. Compared to other Mauna Loa lavas, the submarine lavas have relatively low K/Y and Sr/Y ratios. Low ratios in historical Mauna Loa and Kilauea lavas correlate with periods of higher magma supply and eruption rate. Thus the radial vent lavas may have been erupted during periods when the volcano was more active. Most of Mauna Loa's submarine lavas underwent minor low-pressure crystallization involving olivine followed by plagioclase and clinopyroxene. The 1877 lavas are distinct with orthopyroxene occurring as the second phase to crystallize. This difference in the crystallization sequence is probably related to small differences in bulk composition rather than to variations in extrinsic variables.

Acknowledgments

[53] We thank the Halloween 2002 Mauna Loa expedition science team (including Akel Sterling, Steve Schilling, Marshall Chapman, Mike Vollinger, Kelly Kolysko, and Vickie Bennett), the WHOI National Deep Submergence Facility JASON2 team, and the R/V *T. Thompson* crew for their invaluable help in collecting data and samples for this study, and for subsequent discussions. Mahalo to the Hawaii Mapping Research Group (especially Bruce Applegate) and Nathan Becker for help in processing the EM300 multibeam sonar data, Mike Vollinger for instruction in the black art of XRF analysis, Angie Miller for petrography, and Stephen Blake, Bill Chadwick, Michelle Coombs, Pete Lipman, and Scott Rowland for reviewing this paper. This project was funded by NSF grants OCE-97-29894 to M.G. and OCE-9818744 to J.M.R. This paper is SOEST contribution 6702 and formed part of the M.S. thesis of V. D. Wanless.

References

Abouchami, W., S. Galer, and A. W. Hofmann (2000), High-precision lead isotope systematics of lavas from the Hawaiian Scientific Drilling Project, *Chem. Geol.*, *169*, 187–209.

Applegate, T. B. (1990), Volcanic and structural morphology of the south flank of Axial Volcano, Juan de Fuca Ridge: Results from a Sea MARC I side scan sonar survey, *J. Geophys. Res.*, *95*, 12,795–12,783.

Barnard, W. M. (1995), Mauna Loa Volcano: Historical eruptions, exploration, and observations (1779–1910), in *Mauna Loa Revealed: Structure, Composition, History, and Hazards*, *Geophys. Monogr. Ser.*, vol. 92, edited by J. M. Rhodes and J. P. Lockwood, pp. 1–19, AGU, Washington, D. C.

Blichert-Toft, J., D. Weis, C. Maerschalk, A. Agranier, and F. Albarède (2003), Hawaiian hot spot dynamics as inferred from the Hf and Pb isotope evolution of Mauna Kea volcano, *Geochem. Geophys. Geosyst.*, *4*(2), 8704, doi:10.1029/2002GC000340.

Bridges, N. (1997), Characteristics of seamounts near Hawaii as viewed by GLORIA, *Mar. Geol.*, *138*, 273–301.

Caress, D. W., S. E. Spitzak, and D. N. Chayes (1996), Software for multibeam sonars, *Sea Technol.*, *37*, 54–57.

Chadwick, W. W., and K. A. Howard (1991), The pattern of circumferential and radial eruptive fissures on the volcanoes of Fernandina and Isabela islands, Galapagos, *Bull. Volcanol.*, *53*, 259–275.

Clague, D. A., and J. E. Dixon (2000), Extrinsic controls on the evolution of Hawaiian ocean island volcanoes, *Geochem. Geophys. Geosyst.*, *1*(4), doi:10.1029/1999GC000023.

Clague, D., J. G. Moore, and J. R. Reynolds (2000), Formation of flat-topped volcanic cones in Hawai'i, *Bull. Volcanol.*, *62*, 214–233.

Craig, J. D., J. E. Andrews, and M. A. Meylan (1982), Ferromanganese deposits in the Hawaiian Archipelago, *Mar. Geol.*, *45*, 127–157.

Davis, M. G., M. O. Garcia, and P. Wallace (2003), Volatiles in glasses from Mauna Loa Volcano, Hawai'i: Implications for magma degassing and contamination, and growth of Hawaiian volcanoes, *Contrib. Mineral. Petrol.*, *144*, 570–591.

Eisele, J., W. Abouchami, S. J. G. Galer, and A. W. Hofmann (2003), The 320 kyr Pb isotope evolution of Mauna Kea lavas recorded in the HSDP-2 drill core, *Geochem. Geophys. Geosyst.*, *4*(5), 8710, doi:10.1029/2002GC000339.

Fiske, R. S., and E. D. Jackson (1972), Orientation and growth of Hawaiian volcanic rifts: The effect of regional structure and gravitational stresses, *Proc. R. Soc. London, Ser. A*, *329*, 299–326.

Fornari, D. J. (1986), The geomorphic and structural development of Hawaiian submarine rift zones, *U.S. Geol. Surv. Prof. Pap.*, *1350*, 125–132.

Fornari, D. J., and J. F. Campbell (1987), Submarine topography around the Hawaiian Islands, *U.S. Geol. Surv. Prof. Pap.*, *1350*, 109–124.

Fornari, D. J., A. Malahoff, and B. C. Heezen (1979), Submarine slope micromorphology and volcanic substructure of the island of Hawaii inferred from visual observations made from U.S. Navy Deep Submergence Vehicle (DSV) SEA CLIFF, *Mar. Geol.*, *32*, 1–20.

Fornari, D. J., A. Malahoff, J. P. Lockwood, P. W. Lipman, and M. Rawson (1980), Submarine volcanic features west of Kealakekua Bay, Hawaii, *J. Volcanol. Geotherm. Res.*, *7*, 323–327.

Garcia, M. O. (1996), Petrography, olivine and glass chemistry of lavas from the Hawaii Scientific Drilling Project, *J. Geophys. Res.*, *101*, 11,701–11,713.

Garcia, M. O., and M. G. Davis (2001), Submarine growth and internal structure of oceanic island volcanoes based on submarine observations of Mauna Loa Volcano, Hawaii, *Geology*, *29*, 163–166.

Garcia, M. O., D. Muenow, K. Aggrey, and J. O'Neil (1989), Major element, volatile and stable isotope geochemistry of Hawaiian submarine glasses, *J. Geophys. Res.*, *94*, 10,525–10,538.

Garcia, M. O., T. Hulsebosch, and J. M. Rhodes (1995), Olivine-rich submarine basalts from the southwest rift zone of Mauna Loa Volcano: Implications for magmatic processes and geochemical evolution, in *Mauna Loa Revealed: Structure, Composition, History, and Hazards*, *Geophys. Monogr. Ser.*, vol. 92, edited by J. M. Rhodes and J. P. Lockwood, pp. 219–239, AGU, Washington, D. C.

Gardner, J. V., and J. E. Hughes Clarke (1998), Cruise Report R/V Ocean Alert Cruise A1-98-HW: Mapping the Hawaiian insular slopes, *U.S. Geol. Surv. Open File Rep.*, *98-212*, 27 pp.

Ghiorso, M. S., and R. O. Sack (1995), Chemical mass transfer in magmatic processes. IV. A revised and internally consistent thermodynamic model for the interpolation and extrapolation of liquid-solid equilibria in Magmatic systems at elevated temperatures and pressures, *Contrib. Mineral. Petrol.*, *119*, 197–212.

Gregg, T. K. P., and D. J. Fornari (1998), Long submarine lava flows: Observations and results from numerical modeling, *J. Geophys. Res.*, *103*, 27,517–27,531.

Guillou, H., M. O. Garcia, and L. Turpin (1997), Unspiked K-Ar dating of young volcanic rocks from Loihi and Pitcairn hot spot seamounts, *J. Volcanol. Geotherm. Res.*, *78*, 239–249.

Guth, P. L. (2001), Slope and aspect calculations on gridded digital elevation models: Examples from a geomorphometric toolbox for personal computers, *Z. Geomorphol. N. F. Suppl.*, *101*, 31–52.

Guth, P. L., E. K. Ressler, and T. S. Bacastow (1987), Microcomputer program for manipulating large digital terrain models, *Comput. Geosci.*, *13*, 209–213.

Hagen, R. A., N. A. Baker, D. F. Naar, and R. N. Hey (1990), A SeaMARC II survey of recent submarine volcanism near Easter Island, *Mar. Geophys. Res.*, *12*, 297–315.

Haymon, R. M., et al. (1991), Volcanic eruption of the mid-ocean ridge along the East Pacific Rise crest at 9°45–52′N: Direct submersible observations of seafloor phenomena associated with an eruption event in April, 1991, *Earth Planet. Sci. Lett.*, *119*, 85–101.

Hughes Clarke, J. E., L. A. Mayer, and D. E. Wells (1996), Shallow-water imaging multibeam sonars: A new tool for investigating seafloor processes in the coastal zone and on the continental shelf, *Mar. Geophys. Res.*, *18*, 607–629.

Hughes Clarke, J. E., J. V. Fardner, M. E. Torresan, and L. A. Mayer (1998), The limits of spatial resolution achievable using a 30-kHz multibeam sonar: Model predictions and field results, in *Oceans 98 IEEE OES Conference Proceedings*, pp. 1823–1827, Inst. of Electr. and Electron. Eng., New York.

Jochum, K. P., and S. P. Verma (1996), Extreme enrichment of Sb, Ti and other trace elements in altered MORB, *Chem. Geol.*, *130*, 289–299.

Kauahikaua, J., T. Hildenbrand, and M. Webring (2000), Deep magmatic structures of Hawaiian volcanoes, imaged by three-dimensional gravity models, *Geology*, *28*, 883–886.

Kongsberg Maritime (1997), EM 300 30 kHz multibeam echo sounder for depths reaching 5000 meters, product specifications report, Horten, Norway. (Available at http://www.km.kongsberg.com/KS/WEB/NOKBG0397.nsf/AllWeb/CC966BA500A99CFBC1256C39003DC7BF/$file/160765ad_EM300_Product_specific_lr.pdf ?OpenElement)

Kurz, M. D., and D. P. Kammer (1991), Isotopic evolution of Mauna Loa Volcano, *Earth Planet. Sci. Lett.*, *103*, 257–269.

Kurz, M. D., T. C. Kenna, and D. P. Kammer (1995), Isotopic evolution of Mauna Loa volcano: A view from the submarine southwest rift zone, in *Mauna Loa Revealed: Structure, Composition, History, and Hazards*, *Geophys. Monogr. Ser.*, vol. 92, edited by J. M. Rhodes and J. P. Lockwood, pp. 289–306, AGU, Washington, D. C.

Kurz, M. D., J. Curtice, D. E. Lott, III, and A. Solow (2004), Rapid helium isotopic variability in Mauna Kea shield lavas from the Hawaiian Scientific Drilling Project, *Geochem. Geophys. Geosyst.*, *5*, Q04G14, doi:10.1029/2002GC000439.

Lanphere, M. A., and F. A. Frey (1987), Geochemical evolution of Kohala volcano, *Contrib. Mineral. Petrol.*, *95*, 100–113.

Lipman, P. W. (1980), Rates of volcanic activity along the southwest rift zone of Mauna Loa volcano, Hawaii, *Bull. Volcanol.*, *43*, 703–725.

Lipman, P. W. (1995), Declining growth of Mauna Loa during the last 100,000 years: Rates of lava accumulation vs. gravitational subsidence, in *Mauna Loa Revealed: Structure, Composition, History, and Hazards*, *Geophys. Monogr. Ser.*, vol. 92, edited by J. M. Rhodes and J. P. Lockwood, pp. 45–80, AGU, Washington, D. C.

Lockwood, J. P. (1995), Mauna Loa eruptive history: The preliminary radiocarbon record, in *Mauna Loa Revealed: Structure, Composition, History, and Hazards*, *Geophys. Monogr. Ser.*, vol. 92, edited by J. M. Rhodes and J. P. Lockwood, pp. 81–94, AGU, Washington, D. C.

Lockwood, J. P., and P. W. Lipman (1987), Holocene eruptive history of Mauna Loa Volcano, *U.S. Geol. Surv. Prof. Pap.*, *1350*, 509–535.

Lockwood, J. P., J. J. Dvorak, T. T. English, R. Y. Koyanagi, A. T. Okamura, M. L. Summers, and W. R. Tanigawa (1987), Mauna Loa 1974–1984: A decade of intrusive and extrusive activity, *U.S. Geol. Surv. Prof. Pap.*, *1350*, 537–570.

Mathez, E. A. (1976), Sulfur solubility and magmatic sulfides in submarine basalt glass, *J. Geophys. Res.*, *81*, 4269–4276.

McDonough, W. F., and S. Sun (1995), The composition of the Earth, *Chem. Geol.*, *120*, 223–253.

McMurtry, G. M., E. Herrero-Bervera, M. D. Cremer, J. R. Smith, J. Resig, C. Sherman, and M. E. Torresan (1999),

Stratigraphic constraints on the timing and emplacement of the Alika 2 giant Hawaiian submarine landslide, *J. Volcanol. Geotherm. Res.*, *94*, 35–58.

Montierth, C., A. D. Johnston, and K. V. Cashman (1995), An empirical glass-composition-based geothermometer for Mauna Loa lavas, in *Mauna Loa Revealed: Structure, Composition, History, and Hazards*, *Geophys. Monogr. Ser.*, vol. 92, edited by J. M. Rhodes and J. P. Lockwood, pp. 207–217, AGU, Washington, D. C.

Moore, J. G., and W. W. Chadwick (1995), Offshore geology of Mauna Loa and adjacent areas, Hawaii, in *Mauna Loa Revealed: Structure, Composition, History, and Hazards*, *Geophys. Monogr. Ser.*, vol. 92, edited by J. M. Rhodes and J. P. Lockwood, pp. 21–44, AGU, Washington, D. C.

Moore, J. G., and D. A. Clague (1987), Coastal lava flows from Mauna Loa and Hualalai volcanoes, Kona, Hawaii, *Bull. Volcanol.*, *49*, 752–764.

Moore, J. G., and D. A. Clague (1992), Volcanic growth and evolution of the island of Hawaii, *Geol. Soc. Am. Bull.*, *104*, 1471–1484.

Moore, J. G., and D. Clague (2004), Hawaiian submarine manganese-iron oxide crusts—A dating tool?, *Geol. Soc. Am. Bull.*, *116*, 337–347.

Moore, J. G., and B. P. Fabbi (1971), An estimate of the juvenile sulfur content of basalt, *Contrib. Mineral. Petrol.*, *33*, 118–127.

Moore, J. G., and R. S. Fiske (1969), Volcanic substructure inferred from dredge samples and ocean-bottom photographs, Hawaii, *Geol. Soc. Am. Bull.*, *80*, 1191–1201.

Moore, J. G., D. J. Fornari, and D. A. Clague (1985), Basalts from the 1877 submarine eruption of Mauna Loa, Hawaii: New data on the variation of palagonitization rate with temperature, *U.S. Geol. Surv. Bull.*, *1663*, 1–11.

Moore, J. G., W. R. Normark, and B. J. Szabo (1990), Reef growth and volcanism on the submarine southwest rift zone of Mauna Loa, Hawaii, *Bull. Volcanol.*, *52*, 375–380.

Naumann, T. R., and D. J. Geist (2000), Physical volcanology and structural development of Cerro Azul Volcano, Isabela Island, Galapagos: Implications for the development of Galapagos-type shield volcanoes, *Bull. Volcanol.*, *61*, 497–514.

Norman, M. D., W. L. Griffin, N. J. Pearson, M. O. Garcia, and S. Y. O'Reilly (1998), Quantitative analysis of trace element abundances in glasses and minerals: A comparison of laser ablation ICPMS, solution ICPMS, proton microprobe, and electron microprobe data, *J. Anal. At. Spectrom.*, *13*, 477–482.

Normark, W. R., P. Lipman, J. P. Lockwood, and J. G. Moore (1979), Bathymetric and geologic maps of Kealakekua Bay, Hawaii, *U.S. Geol. Surv. Misc. Field Stud. Map*, *MF-986*.

Ode, H. (1957), Mechanical analysis of the dike pattern of the Spanish Peaks area, Colorado, *Geol. Soc. Am. Bull.*, *68*, 567–576.

Pietruszka, A. J., and M. O. Garcia (1999), A rapid fluctuation in the mantle source and melting history of Kilauea volcano inferred from the geochemistry of its historical summit lavas (1790–1982), *J. Petrol.*, *40*, 1321–1342.

Pollard, D. D. (1987), Elementary fracture mechanics applied to the structural interpretation of dykes, *Geol. Soc. Am. Bull.*, *93*, 1291–1303.

Rappaport, Y., D. F. Naar, C. C. Barton, Z. J. Lui, and R. N. Hey (1997), Morphology and distribution of seamounts surrounding Easter Island, *J. Geophys. Res.*, *102*, 24,713–24,728.

Rhodes, J. M. (1995), The 1852 and 1868 Mauna Loa picrite eruptions: Clues to parental magma compositions and the magmatic plumbing system, in *Mauna Loa Revealed: Structure, Composition, History, and Hazards*, *Geophys. Monogr. Ser.*, vol. 92, edited by J. M. Rhodes and J. P. Lockwood, pp. 241–262, AGU, Washington, D. C.

Rhodes, J. M., and S. R. Hart (1995), Episodic trace element and isotopic variations in historical Mauna Loa lavas: Implications for magma and plume dynamics, in *Mauna Loa Revealed: Structure, Composition, History, and Hazards*, *Geophys. Monogr. Ser.*, vol. 92, edited by J. M. Rhodes and J. P. Lockwood, pp. 263–288, AGU, Washington, D. C.

Rhodes, J. M., and M. J. Vollinger (2004), Composition of basaltic lavas sampled by phase-2 of the Hawaii Scientific Drilling Project: Geochemical stratigraphy and magma types, *Geochem. Geophys. Geosyst.*, *5*, Q03G13, doi:10.1029/2002GC000434.

Robinson, J., and B. W. Eakins (2006), Calculated volumes of individual shield volcanoes at the young end of the Hawaiian Ridge, *J. Volcanol. Geotherm. Res.*, in press.

Rowland, S. K., and G. P. Walker (1990), Pahoehoe and aa in Hawaii: Volumetric flow rate controls the lava structure, *Bull. Volcanol.*, *52*, 615–628.

Rubin, A. M. (1990), A comparison of rift-zone tectonics in Iceland and Hawaii, *Bull. Volcanol.*, *52*, 302–319.

Scaillet, S., and H. Guillou (2004), A critical evaluation of young (near zero) K-Ar Ages, *Earth Planet. Sci. Lett.*, *220*, 265–275.

Sharp, W. D., and P. R. Renne (2005), The $^{40}Ar/^{39}Ar$ dating of core recovered by the Hawaii Scientific Drilling Project (phase 2), Hilo, Hawaii, *Geochem. Geophys. Geosyst.*, *6*, Q04G17, doi:10.1029/2004GC000846.

Stearns, H. T., and G. A. Macdonald (1946), *Geology and Ground-Water Resources of the Island of Hawaii*, 363 pp., *Bull. 9*, Div. of Hydrogr., Terr. of Hawaii, Honolulu.

Swanson, D. A., W. A. Duffield, and R. S. Fiske (1976), Displacement of the south flank of Kilauea Volcano: The result of forceful intrusion of magma into the rift zones, *U.S. Geol. Surv. Prof. Pap.*, *963*, 1–39.

Walker, G. P. (1990), Geology and volcanology of the Hawaiian Islands, *Pac. Sci.*, *44*, 315–347.

Walker, G. P. (1993), Basaltic-volcano systems*Geol. Soc. Spec. Publ.*, *73*, 3–38.

Wanless, V. D., M. O. Garcia, J. M. Rhodes, D. Weis, and M. D. Norman (2006), Shield stage volcanism on Mauna Loa Volcano, Hawai'i, *J. Volcanol. Geotherm. Res.*, in press.

Weis, D., and F. A. Frey (2002), Submarine basalts of the Northern Kerguelen Plateau: Interaction between the Kerguelen Plume and the Southeast Indian ridge revealed at ODP site 1140, *J. Petrol.*, *43*, 1287–1309.

Weis, D., B. Kieffer, C. Maerschalk, W. Pretorius, and J. Barling (2005), High-precision Pb-Sr-Nd-Hf isotopic characterization of USGS BHVO-1 and BHVO-2 reference materials, *Geochem. Geophys. Geosyst.*, *6*, Q02002, doi:10.1029/2004GC000852.

Wessel, P., and W. H. F. Smith (1995), New version of the Generic Mapping Tools released, *Eos Trans. AGU*, *76*, 329.

Whitney, H. M. (1877), A new and remarkable volcanic outbreak in Kealakakua Bay!, *Hawaii. Gaz.*, *13*, 3.

Wolfe, E. W., and J. Morris (1996), Geologic map of the island of Hawaii, *U.S. Geol. Surv. Misc. Invest. Ser.*, *I-2524*.

Wright, T. L. (1971), Chemistry of Kilauea and Mauna Loa lava in space and time, *U.S. Geol. Surv. Prof. Pap.*, *735*, 1–39.